Flare particle acceleration in the interaction of twisted coronal flux ropes

James Threlfall, *A. W. Hood, P. K. Browning*

jwt9@st-andrews.ac.uk

@JamesWThrelfall

Solar & Magnetospheric Theory Group, University of St Andrews

University of St Andrews

Overview

- Motivation (solar flares)
- Background (reconnection and particle acceleration)
- The test particle approach
- Multi-thread MHD loop cascade/eruption (2 loops)
  - Single loop disruption
  - Single loop disruption triggers secondary destabilisation

Motivation

(New) motivation

credit: Morgan/ Druckmuller

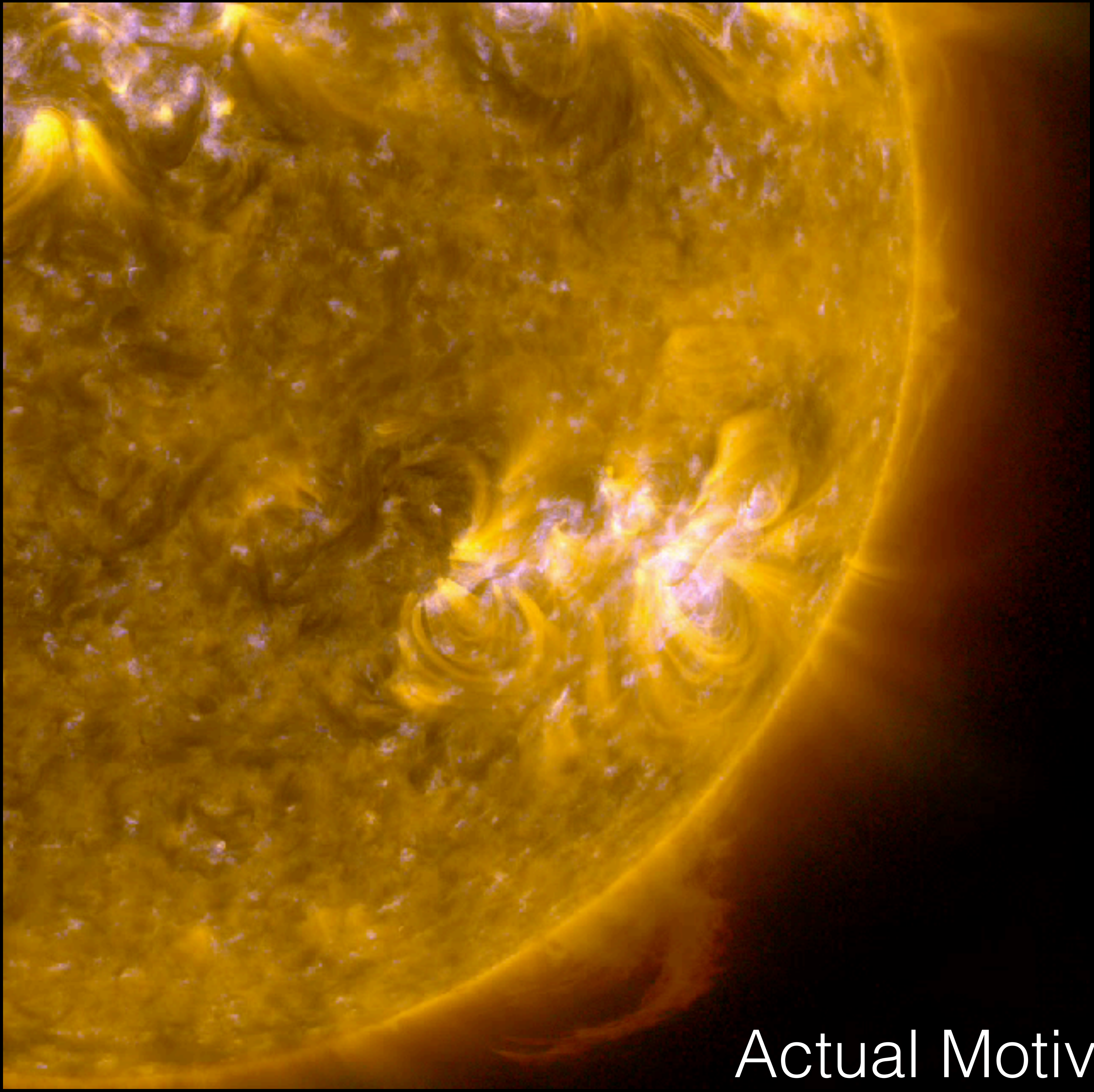

Actual Motivation

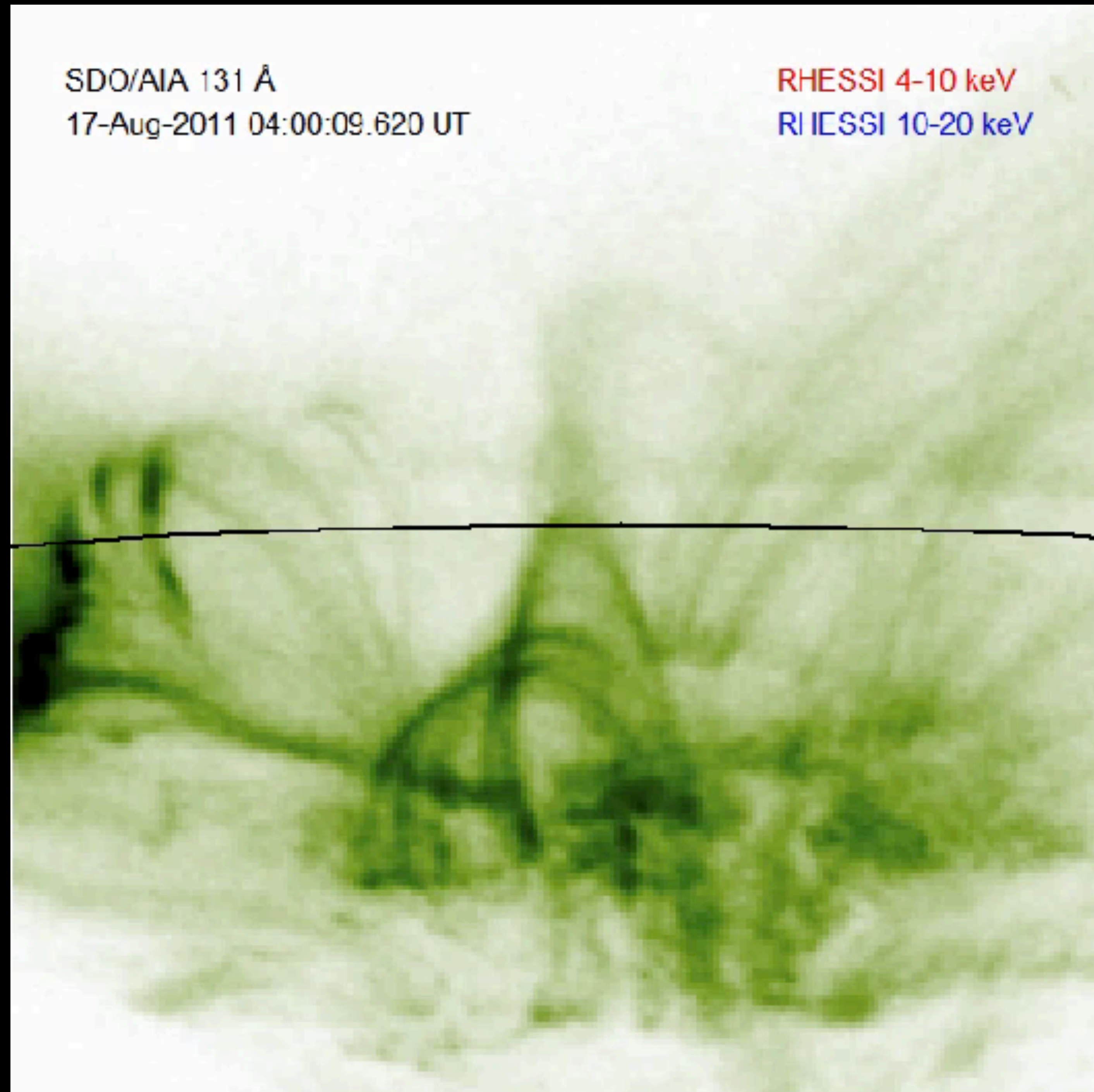

Su et al.,
Nat. Phys. (2013)

- ✦ Clear evidence of **restructuring of magnetic fields** here (and most flares).
- ✦ Tangled/twisted coronal fields "**reconnect**" to relax to lower energy state.
- ✦ Released energy: heats, bulk plasma motion and **accelerates particles**.

Background

3D Magnetic Reconnection

- Reconnection historically studied using 2D steady state models: limitations and properties reasonably well known and understood
- In 3D: **No** fundamental restriction on where reconnection occurs.
- Necessary and sufficient condition for reconnection:

$$\int E_{||} ds \neq 0$$

(e.g. *Schindler et al. 1988; Hesse and Schindler 1988*)

- "Cut and paste" 2D field line picture no longer holds:
  3D reconnection happens continuously and continually within finite volume.

How to model?

- Several ways to model a plasma:
  - ✦ Single fluid (MHD)
    treat plasma as a continuum (i.e., a single fluid) so solve just the one set of fluid equations and Maxwell's equations.
  - ✦ 2-fluid
    Treat electrons and ions as separate continuum (solve the electron & ion fluid equations + Maxwell's equations involving both the electrons and ions).
  - ✦ Kinetic
    Use distribution functions for each particle species & solve for motion of each species.
  - ✦ Individual particles
    For each particle solve for motion due to surrounding magnetic and electric fields.

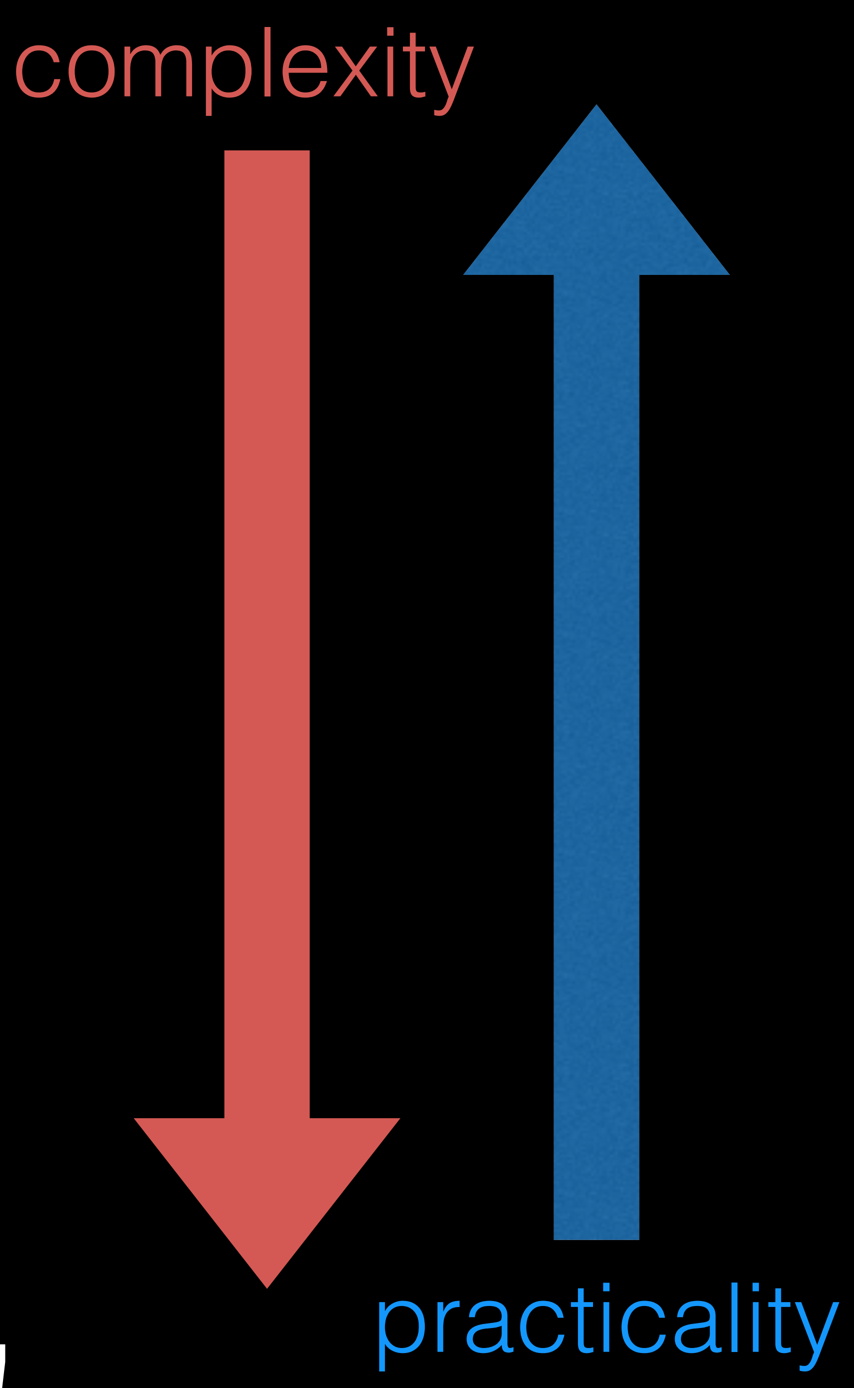

All have advantages and limitations!

Test Particles

- In uniform B-field, particles gyrate orbit field lines with Larmor/gyro-radius:

$$r_g = \frac{mv_\perp}{eB}$$

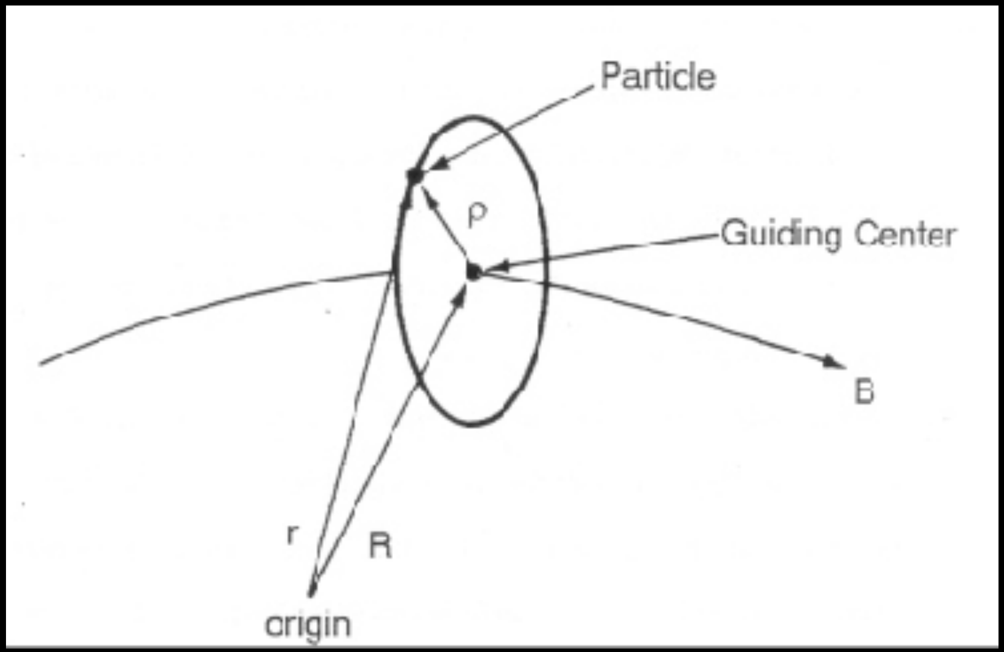

- **Averaging over gyro-motion** ("guiding centre approximation") **reduces complexity** (provided environment does not change during orbit).

- Typically leads to fast parallel motion (particularly when some component of E-field parallel to B) and slower perpendicular drifts.

- Downside: Orbits affected by collisions and back-react upon the fields (solved by e.g. PIC but omitted here - PIC also has big limitations!)

Particle Orbit Equations

Particle guiding centre behaviour (Northrop, 1963)

$$\frac{dv_\parallel}{dt} = \frac{qE_\parallel}{m_0} - \frac{\mu_B}{m_0}\frac{\partial B}{\partial s} + \mathbf{u}_E \cdot \left(\frac{\partial \mathbf{b}}{\partial t} + v_\parallel \frac{\partial \mathbf{b}}{\partial s} + (\mathbf{u}_E \cdot \nabla)\,\mathbf{b} \right), \tag{1a}$$

(1c)

(1a) **Parallel equation of motion** (think $a = F/m$) - if present, $E_\parallel$ typically dominates.

NB. $\mathbf{b} = \frac{\mathbf{B}}{|B|}$, $\mathbf{u_E} = \frac{\mathbf{E} \times \mathbf{b}}{|B|}$, $v_\parallel = \mathbf{v} \cdot \mathbf{b}$, $\mu_B = \frac{mv_g^2}{2B}$ for gyro-velocity v_g,
$s =$ line element along $\mathbf{b}$, particle charge q, mass m.

Particle Orbit Equations

Particle guiding centre behaviour (Northrop, 1963)

$$\frac{dv_\parallel}{dt} = \frac{qE_\parallel}{m_0} - \frac{\mu_B}{m_0}\frac{\partial B}{\partial s} + \mathbf{u}_E \cdot \left(\frac{\partial \mathbf{b}}{\partial t} + v_\parallel \frac{\partial \mathbf{b}}{\partial s} + (\mathbf{u}_E \cdot \nabla)\,\mathbf{b} \right), \tag{1a}$$

$$\begin{aligned} \dot{\mathbf{R}}_\perp = \frac{\mathbf{b}}{B} \times \Bigg[-\mathbf{E} + \frac{\mu_B}{q}\nabla B + \frac{m_0}{q}\Bigg(v_\parallel \frac{\partial \mathbf{b}}{\partial t} + v_\parallel^2 \frac{\partial \mathbf{b}}{\partial s} \\ + v_\parallel (\mathbf{u}_E \cdot \nabla)\,\mathbf{b} + \frac{\partial \mathbf{u}_E}{\partial t} + v_\parallel \frac{\partial \mathbf{u}_E}{\partial s} + (\mathbf{u}_E \cdot \nabla)\,\mathbf{u}_E \Bigg) \Bigg], \end{aligned} \tag{1b}$$

$$\tag{1c}$$

(1a) **Parallel equation of motion** (think $a = F/m$) - if present, $E_\parallel$ typically dominates.

(1b) **Perpendicular drift of guiding centre** (RHS: $E \times B$, ∇B and lower order drifts).

NB. $\mathbf{b} = \frac{\mathbf{B}}{|B|}$, $\mathbf{u_E} = \frac{\mathbf{E} \times \mathbf{b}}{|B|}$, $v_\parallel = \mathbf{v} \cdot \mathbf{b}$, $\mu_B = \frac{m v_g^2}{2B}$ for gyro-velocity v_g,
$s =$ line element along $\mathbf{b}$, particle charge q, mass m.

Particle Orbit Equations

Particle guiding centre behaviour (Northrop, 1963)

$$\frac{dv_\parallel}{dt} = \frac{qE_\parallel}{m_0} - \frac{\mu_B}{m_0}\frac{\partial B}{\partial s} + \mathbf{u}_E \cdot \left(\frac{\partial \mathbf{b}}{\partial t} + v_\parallel \frac{\partial \mathbf{b}}{\partial s} + (\mathbf{u}_E \cdot \nabla)\mathbf{b}\right), \tag{1a}$$

$$\begin{aligned}\dot{\mathbf{R}}_\perp = \frac{\mathbf{b}}{B} \times \Bigg[-\mathbf{E} + \frac{\mu_B}{q}\nabla B + \frac{m_0}{q}\Bigg(v_\parallel \frac{\partial \mathbf{b}}{\partial t} + v_\parallel^2 \frac{\partial \mathbf{b}}{\partial s} \\ + v_\parallel (\mathbf{u}_E \cdot \nabla)\mathbf{b} + \frac{\partial \mathbf{u}_E}{\partial t} + v_\parallel \frac{\partial \mathbf{u}_E}{\partial s} + (\mathbf{u}_E \cdot \nabla)\mathbf{u}_E\Bigg)\Bigg],\end{aligned} \tag{1b}$$

$$\frac{d}{dt}E_K = q\dot{\mathbf{R}} \cdot \mathbf{E} + \mu_B \frac{\partial B}{\partial t}, \qquad E_K = \frac{m_0 {v_\parallel}^2}{2} + \mu_B B + \frac{m_0 {u_E}^2}{2}, \tag{1c}$$

(1a) **Parallel equation of motion** (think $a = F/m$) - if present, $E_\parallel$ typically dominates.

(1b) **Perpendicular drift of guiding centre** (RHS: $E \times B$, ∇B and lower order drifts).

(1c) **Change in KE** via work done by $E-$field on guiding centre and induction effect of time-dependent field.

(1c) **KE divided between parallel, perpendicular and gyro-motion**.

Blatant plug!

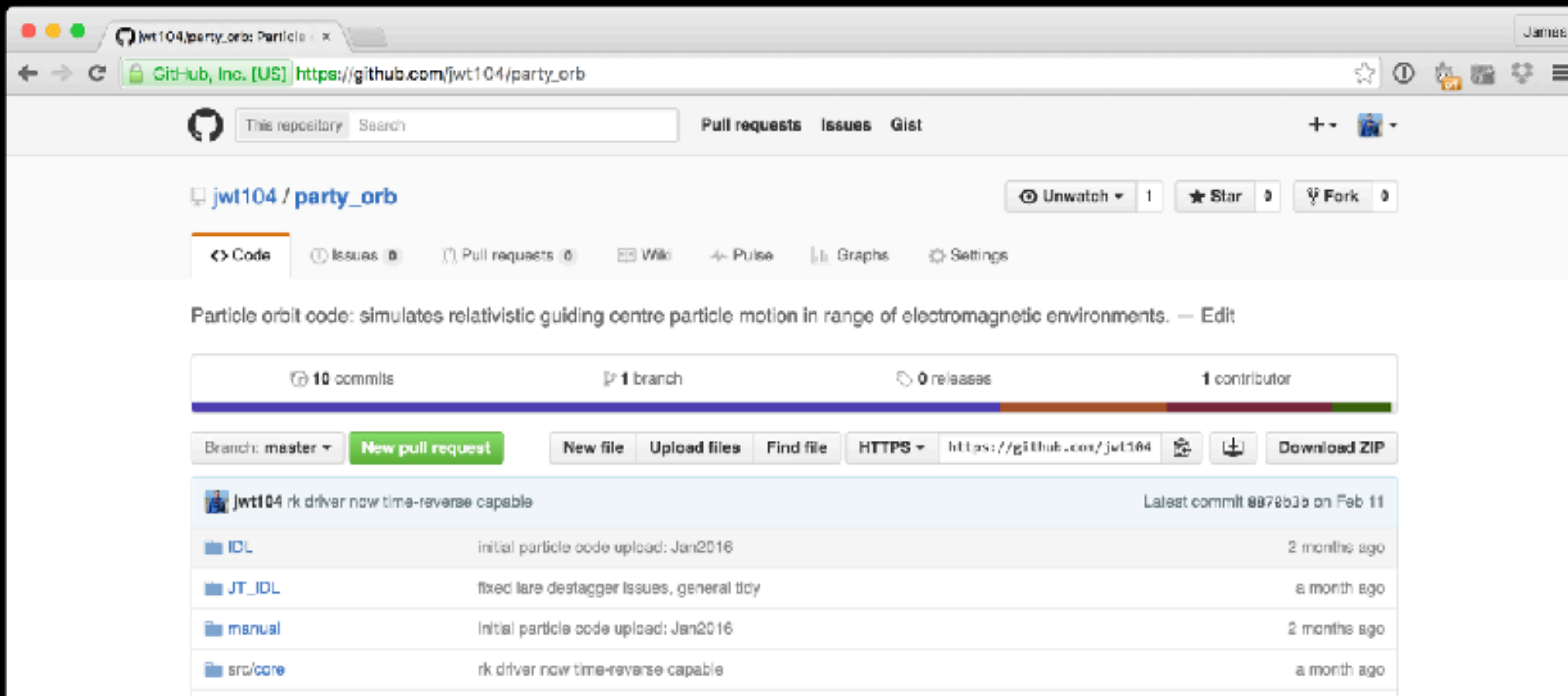

- We use a **relativistic** form of guiding centre equations, solved using 4th order Runge Kutta scheme - only needs **E** and **B**.
- Assumes spatial and temporal scales of gyro-motion and field environment are well separated (checked and also check that $B \neq 0$).
- Adapted to take input from analytical fields or various MHD codes.
- Code available on github: **https://github.com/jwt104/party_orb**

What configurations to probe?

(shameless self-promotion warning)

- Isolated topological features - **separators** (*Threlfall et al. A&A, 2015,2016a*)
- Non-flaring Active Region model (MHD) (*Threlfall et al. A&A, 2016b*)
- Non-topological coronal reconnection model (*Threlfall et al., Solar Physics, 2017*)
- Multi-thread avalanche energy release (MHD) (Threlfall et al., A&A, 2018, accepted)

Brief aside: Energy Scaling

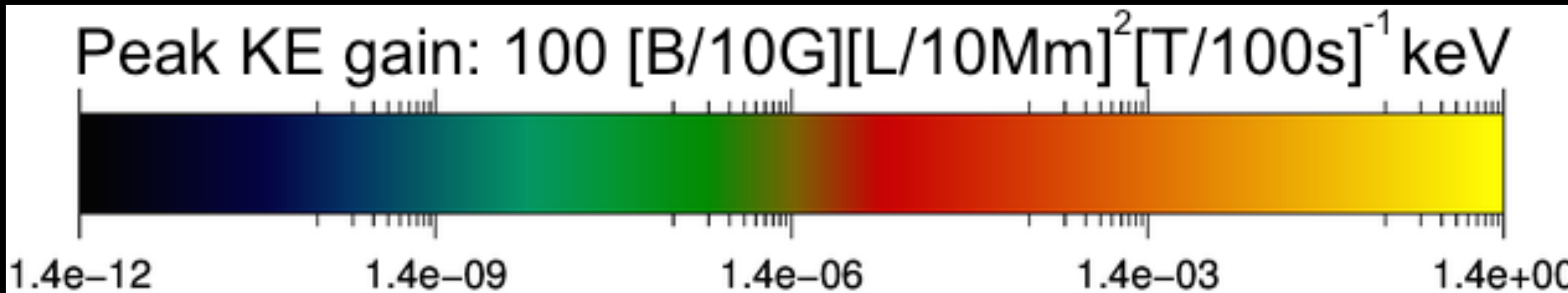

- See e.g. Threlfall et al. (2016)
- Initial analytical/numerical field model often contains **dimensional** AND **non-dimensional scales**.
- Particles accelerated by "field aligned potential difference"
- Resulting energies determined by non-dimensional parameters, THEN scaled by dimensional values
- Can estimate how energy gains will scale

$$\Delta = \int E_{||} ds = \frac{l_{\rm scl}^2 b_{\rm scl}}{t_{\rm scl}} \int \tilde{E}_{||} d\tilde{s}$$
$$= \frac{l_{\rm scl}^2 b_{\rm scl}}{t_{\rm scl}} \tilde{\Delta}.$$

(i.e. 10-fold increase in length should yield 100-fold increase in energy gains!)

Multi-thread avalanche energy release (MHD)
(Threlfall et al., A&A, 2018, accepted)

Multi-thread cascade

- **Tam et al. (2015), Hood et al. (2016)**
- First demo of single coronal loop thread destabilising neighbouring threads, leading to a cascade
- MHD
- Energy release in discrete bursts (nanoflares?)
- Study up to 23 threads

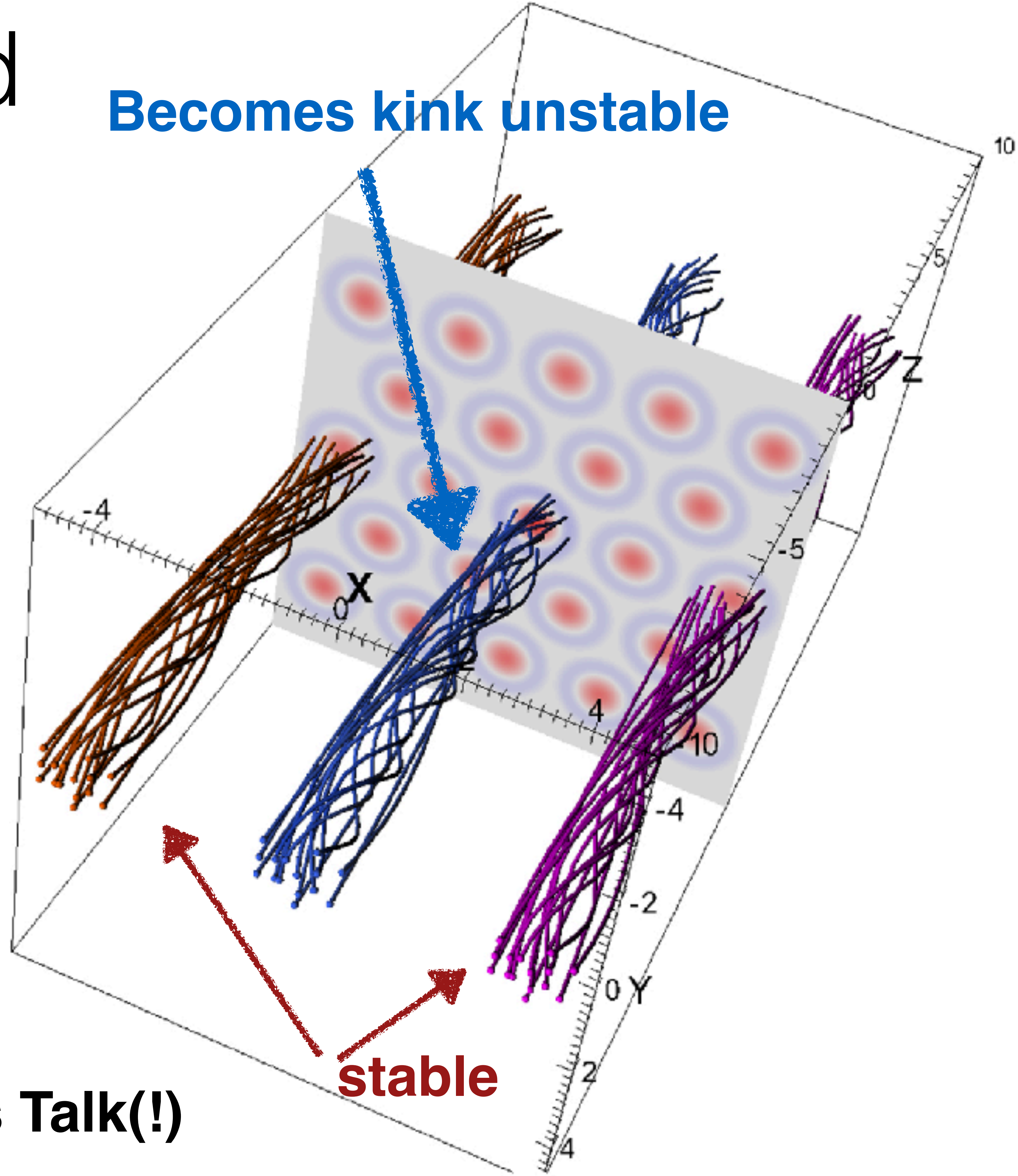

More details: Asad's Talk(!)

Multi-thread cascade

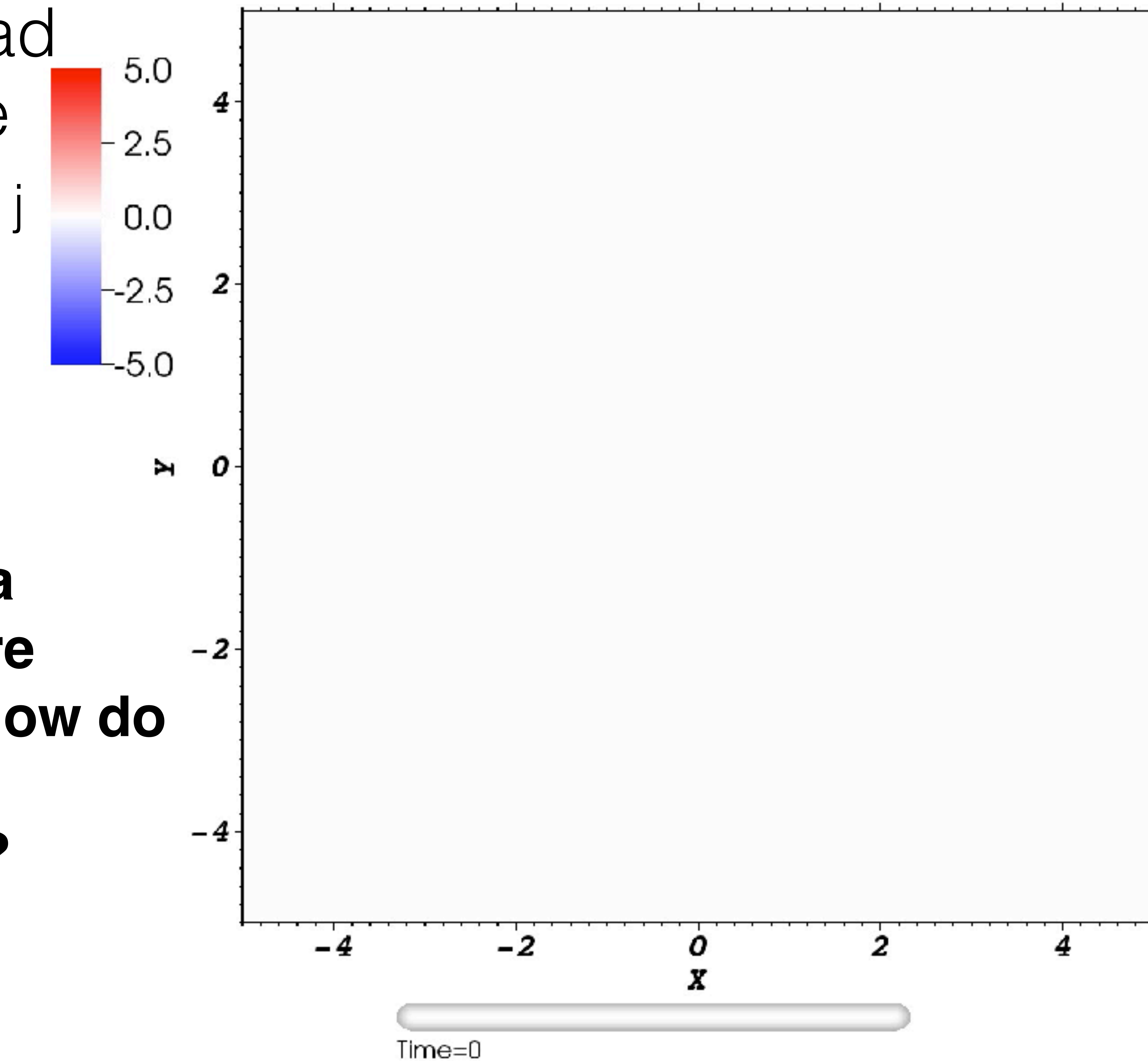

- **If this is a "nanoflare storm", how do particles respond?**

Threlfall et al. (2018, in press.)

Our Study

- First step: Study particle behaviour in two loop config.
- Cases:
    - One loop does not destabilise second loop
    - One loop triggers second loop disruption

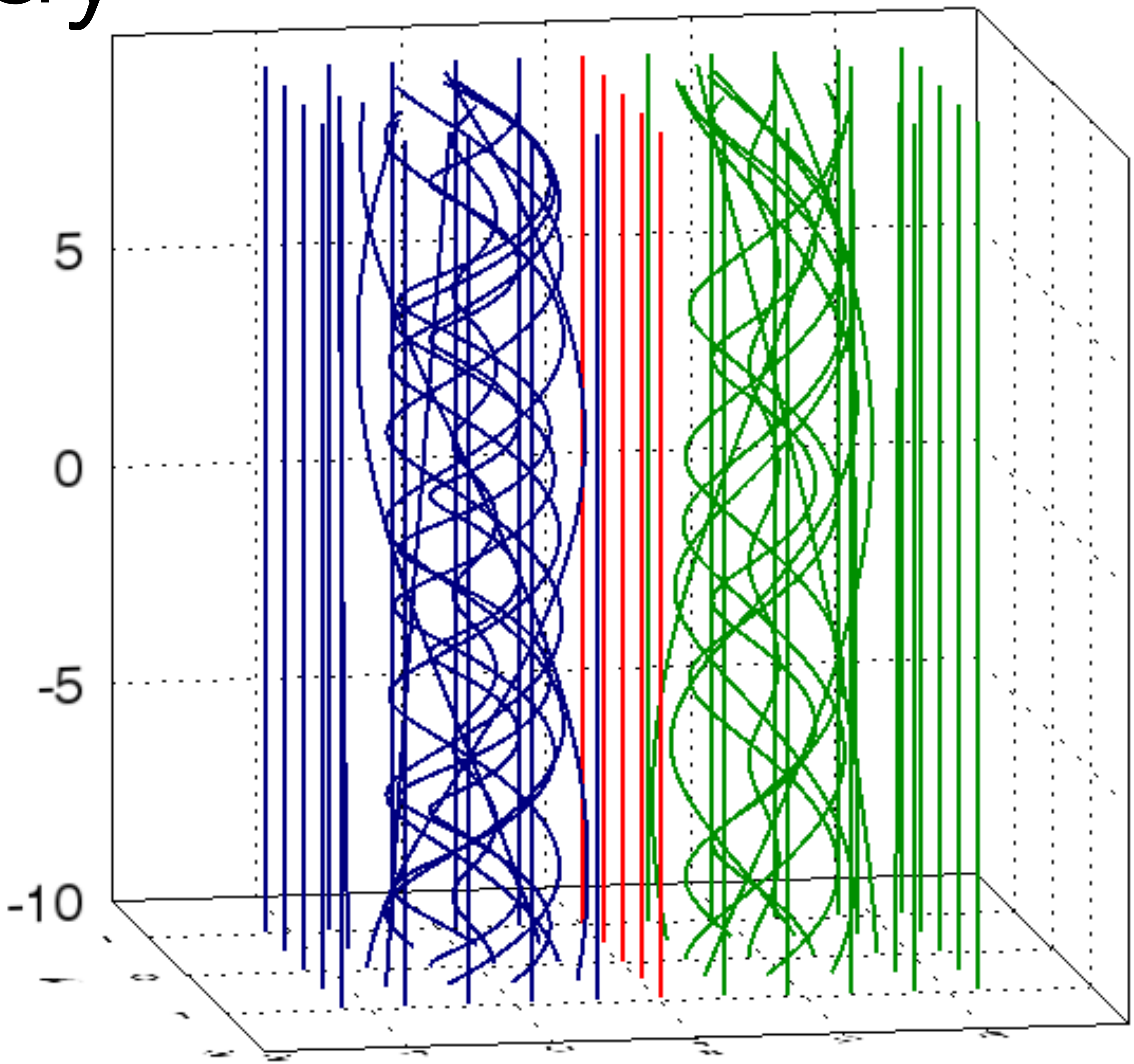

Any Previous? - Gordovskyy et al. (2011, 2012)

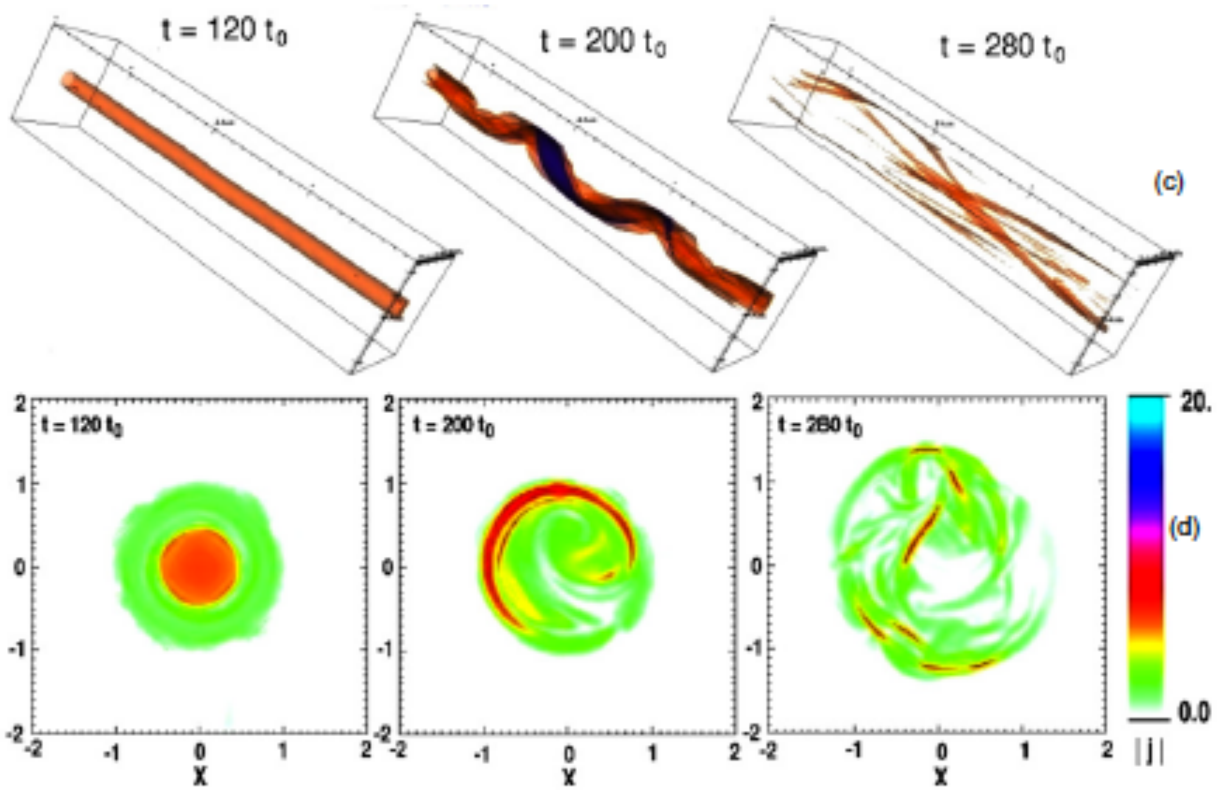

- Gordovskyy et al. (2011, 2012), studied single loop destabilisation using test particles
- How do our final positions and energy distributions compare?

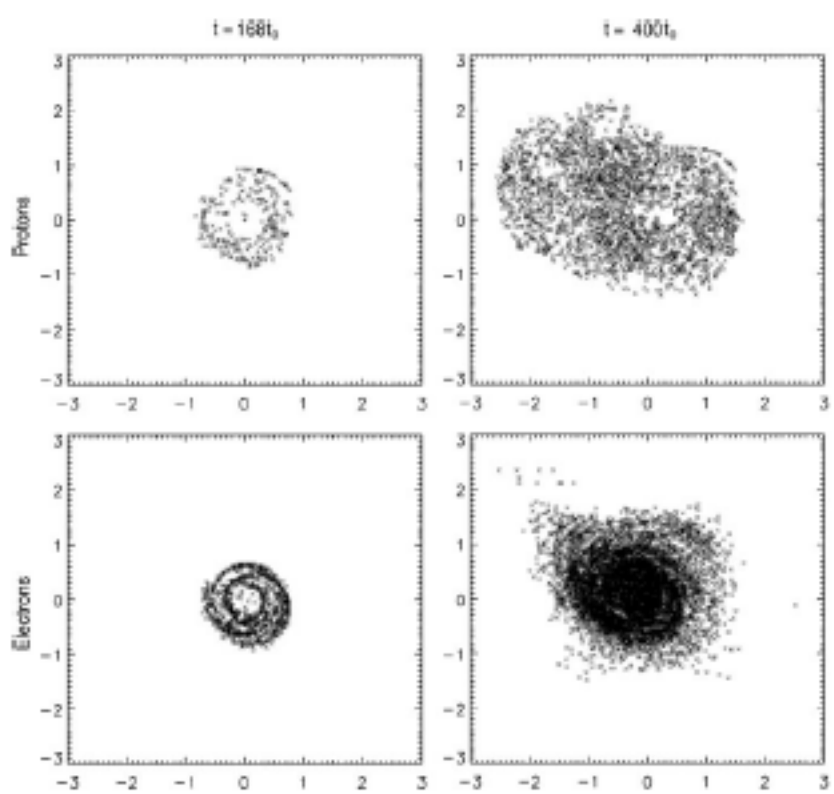

Figure 9 Horizontal distribution of protons and electrons near fluxtube footpoints ($\zeta > 9.0L_0$ and $\zeta < -9.0L_0$) in Model C with the resistivity R1. Left panels ($t = 168t_0$) correspond approximately to the maximum of magnetic energy release, right panels ($t = 400t_0$) correspond to the end of reconnection.

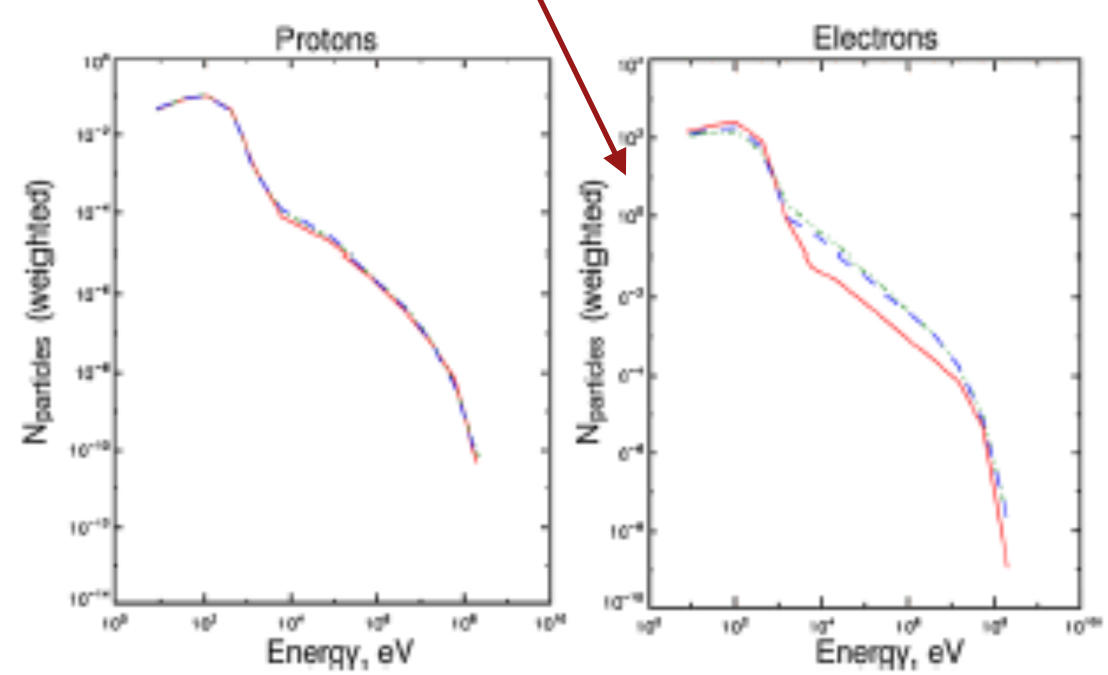

Figure 14 Final proton and electron spectra for Model B with resistivity R1 for fully reflective boundaries (dot-dot-dashed green lines), semi-transparent boundaries (*i.e.* partially reflective boundaries with the artificial loss cone) (dashed blue lines) and fully transparent boundaries (solid red lines).

Case 1

Case 1 - single loop disruption

- Single loop benchmark **(background AND anomalous resistivity acting above j_{crit})**
- Blue loop initially **kink unstable**
- Green initially **marginally stable**
- Can we disentangle the effects of both resistivities?

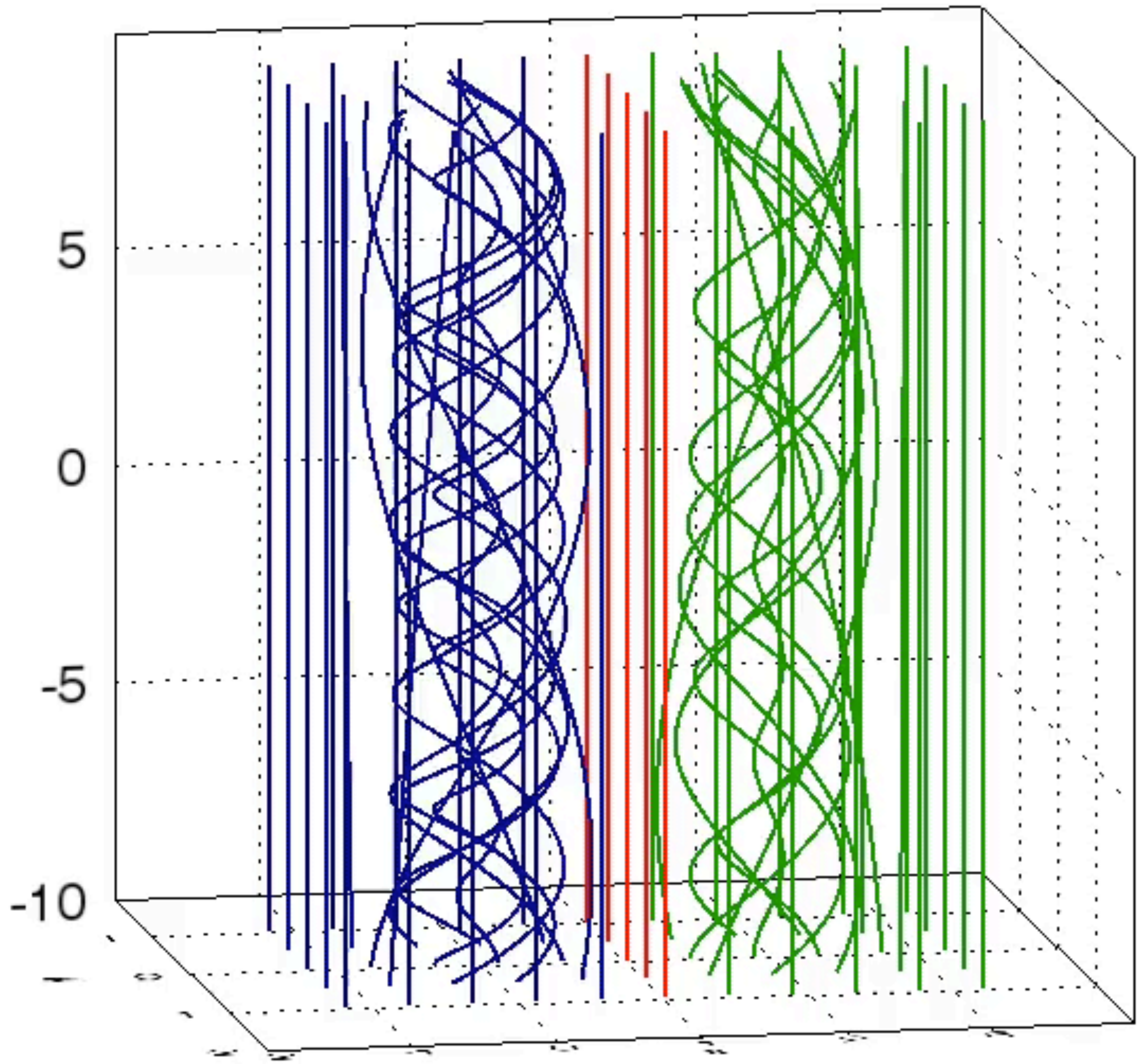

purple = current > j_{crit}

Case 1 - single loop disruption

- Define three phases based on energy changes
- Study particle behaviour in each phase
- Use random initial positions, pitch angles, Maxwellian energies..

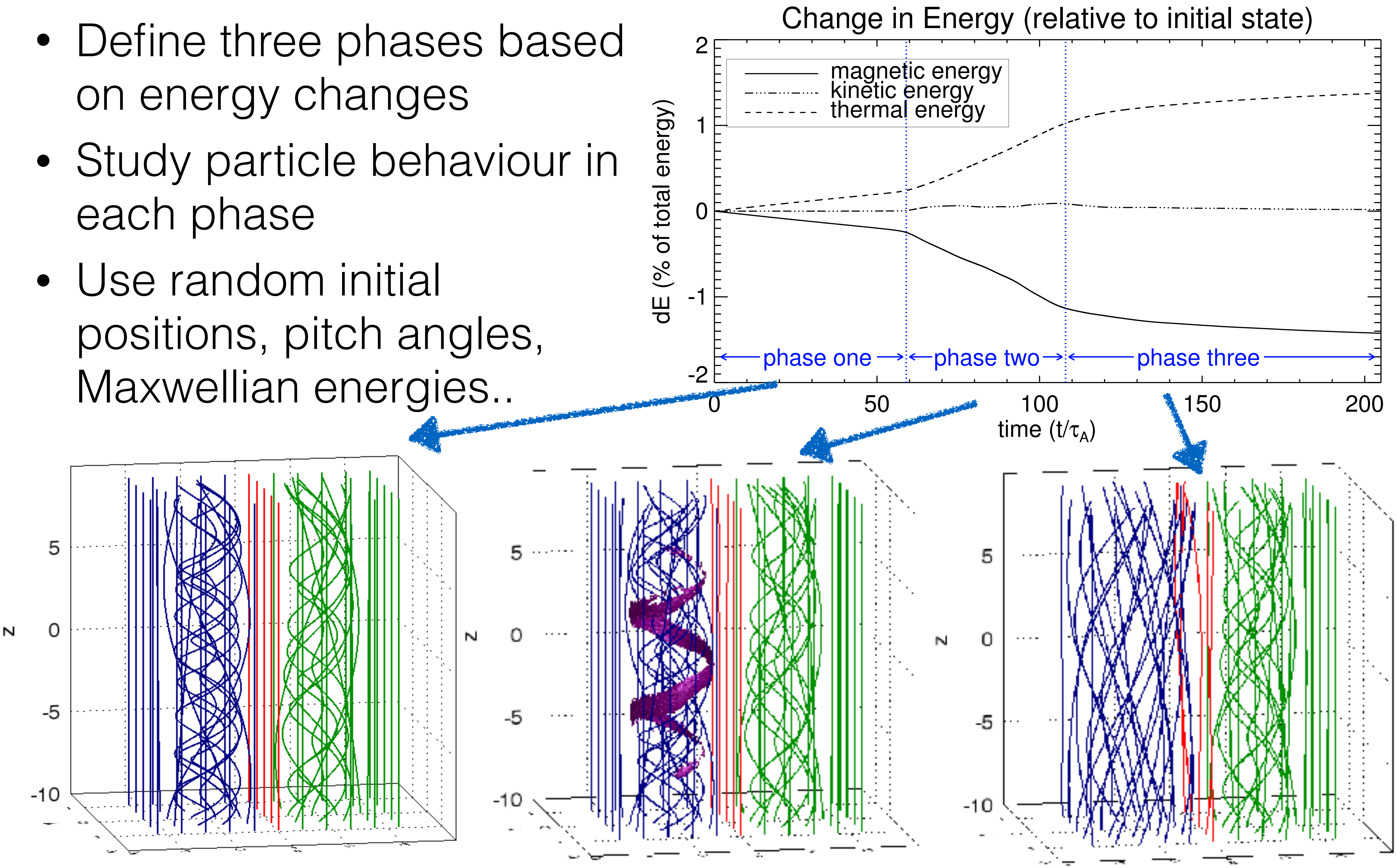

Case 1: Phase 1

$\eta_{bkg} + \eta_{anom}$

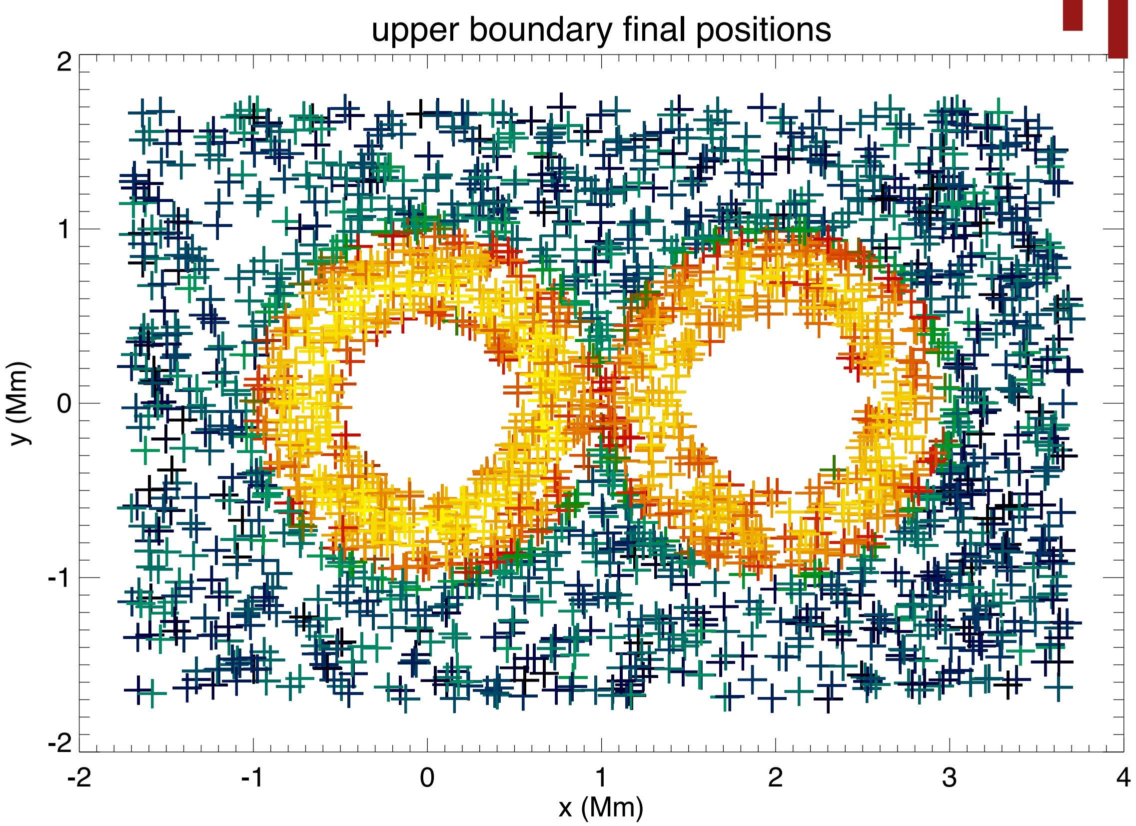

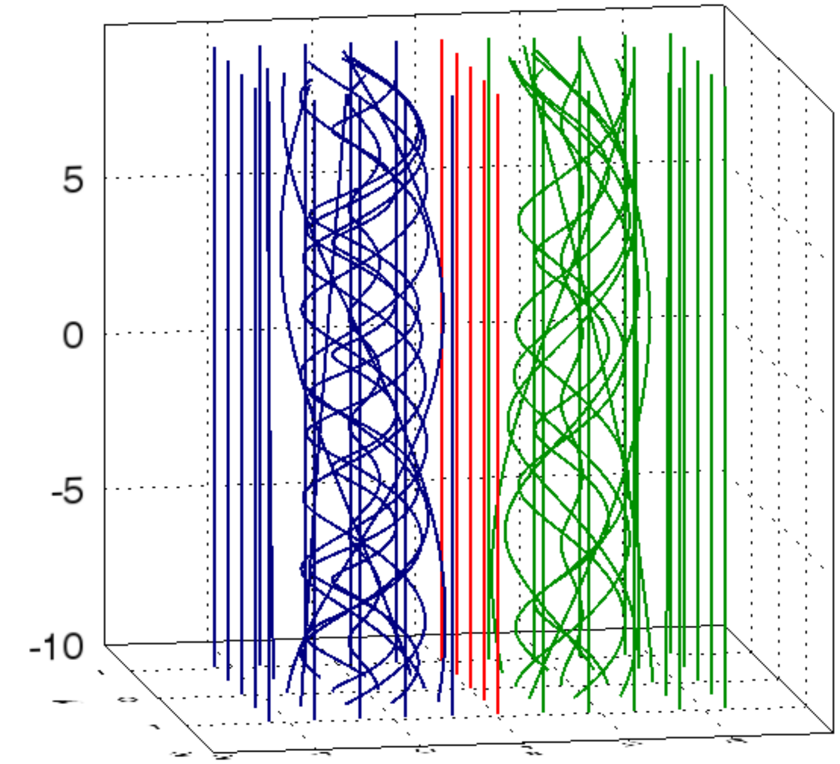

- $j<j_{crit}$ in Phase 1
- η_{bkg} causes acceleration **in both tubes** (even unstable one)
- Weak η_{bkg} and weak current still yield big energy gains over large distances

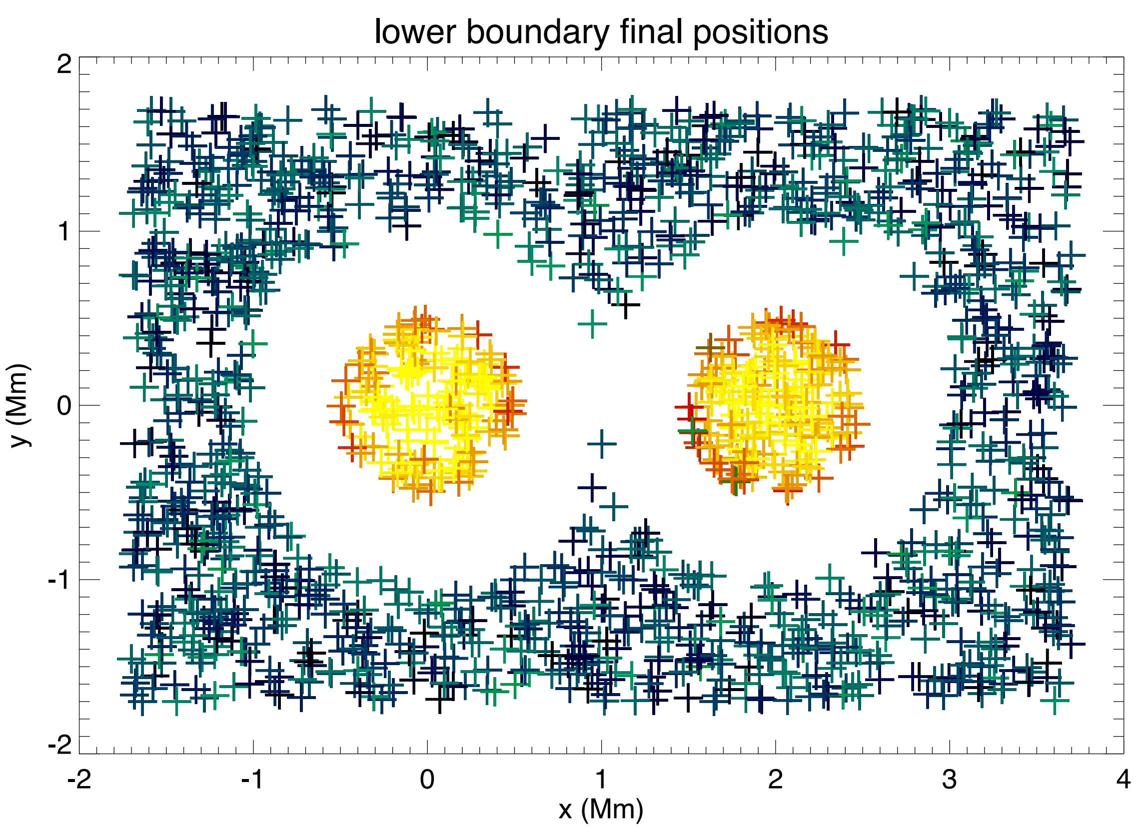

Final boundary positions

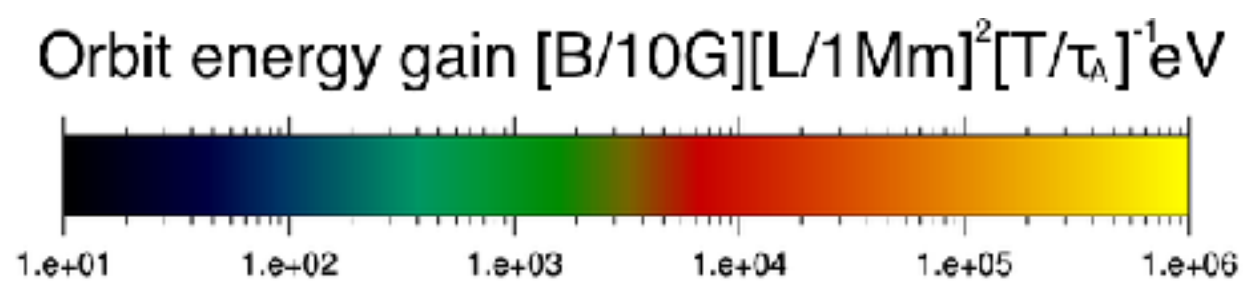

Case 1: Phase 1

~~η_{bkg}~~

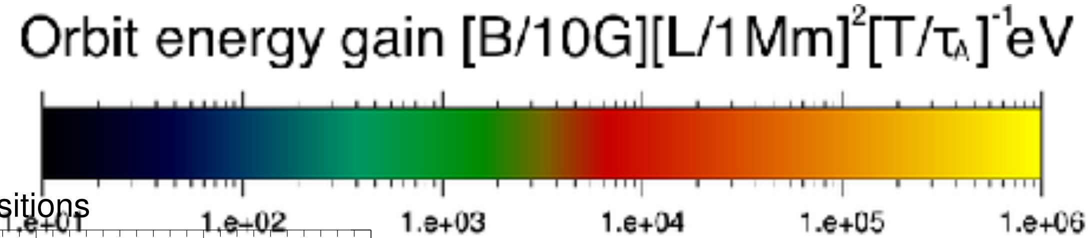

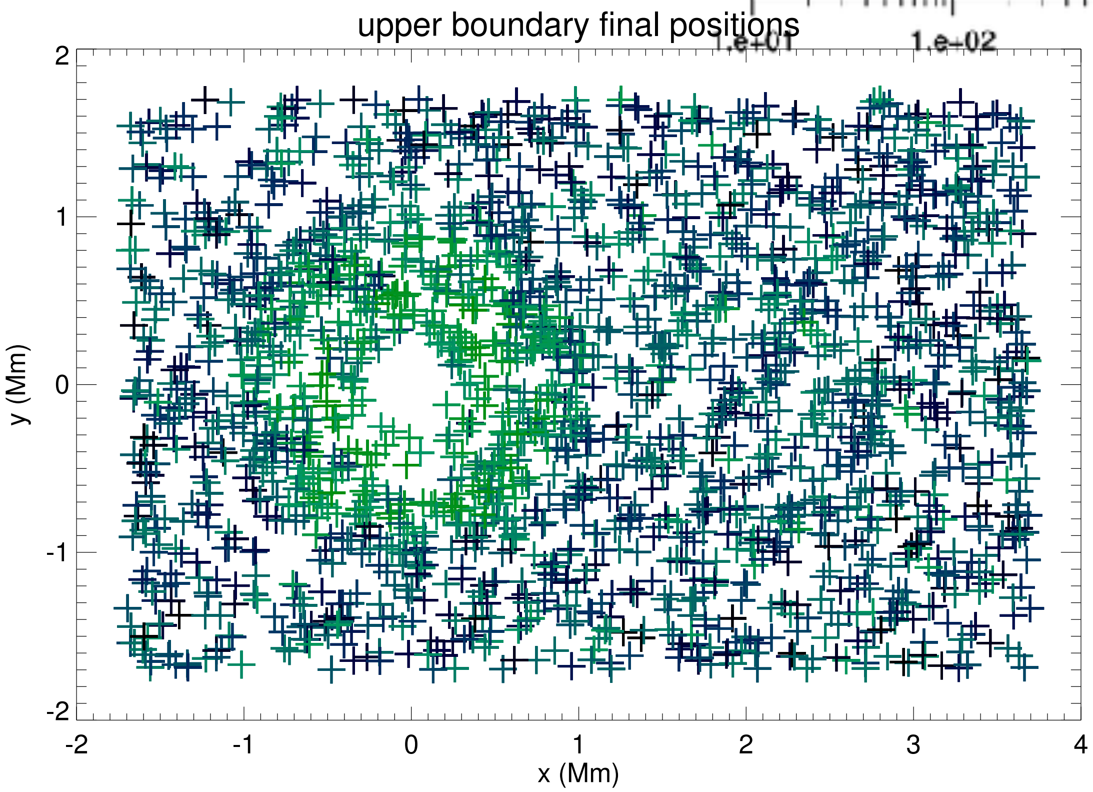

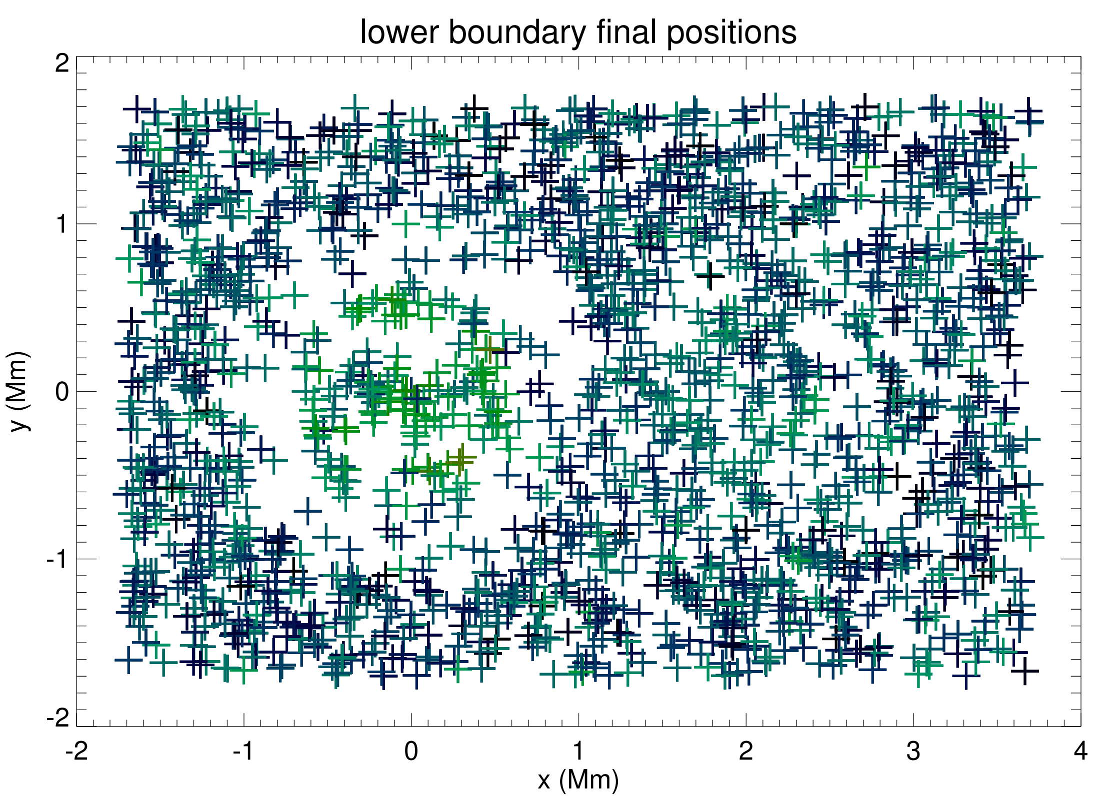

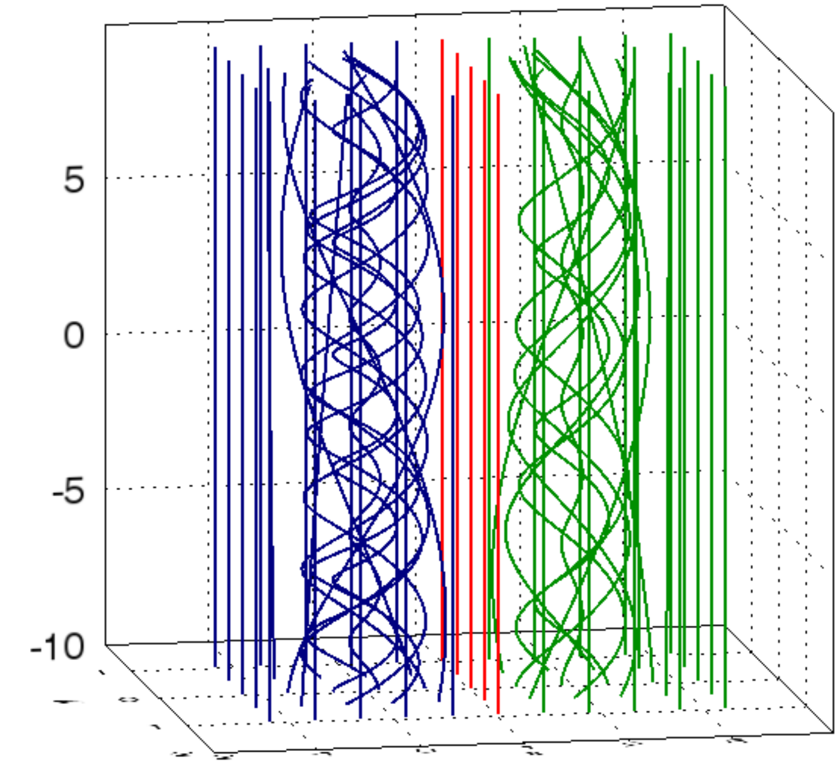

- η_{bkg}=0, little/no accn.
- Energy dist:

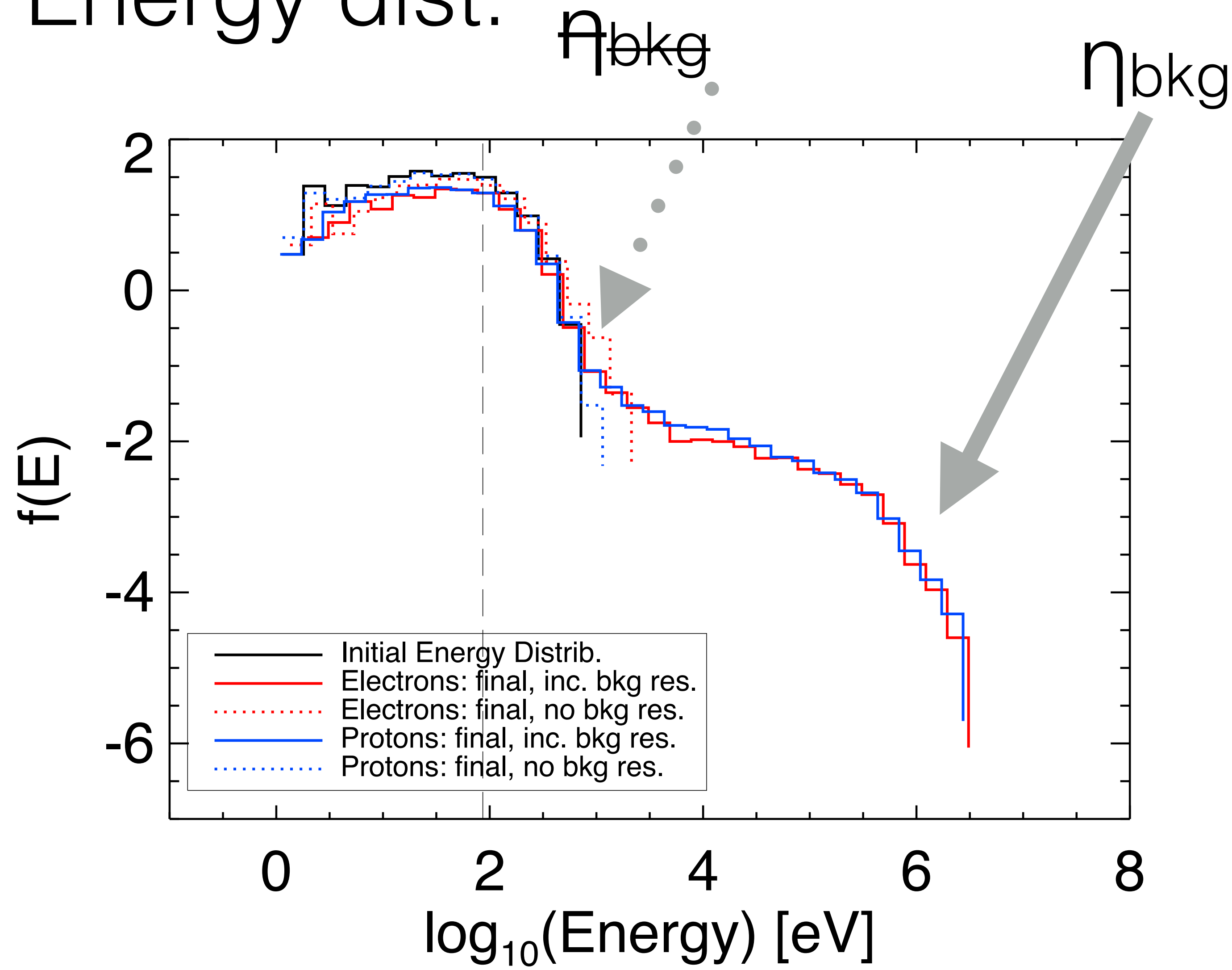

Case 1: Phase 2

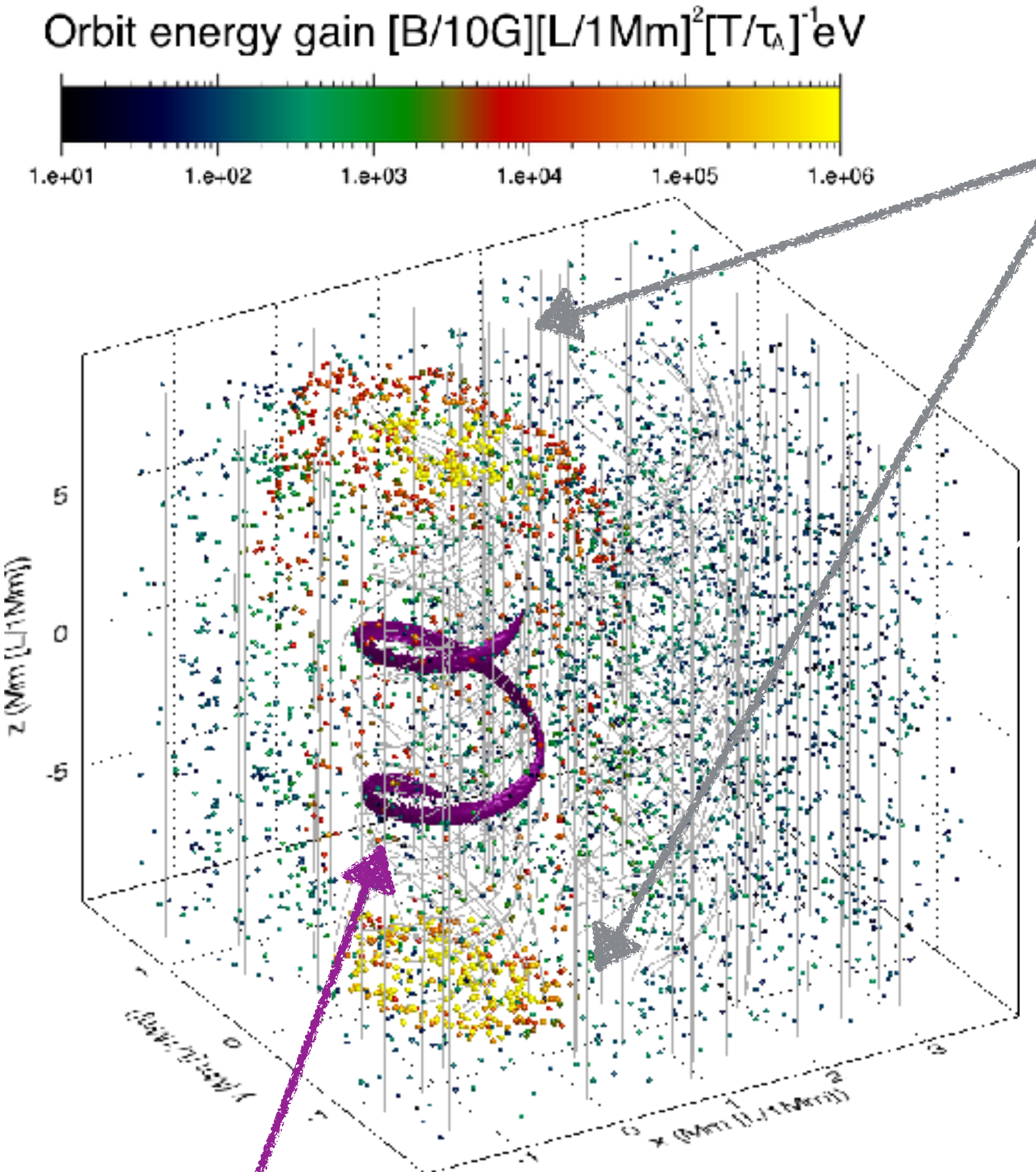

Helical currents >j_{crit}

- Thin beams of accelerated particles at top and bottom boundaries.
- More keV-MeV orbits when including η_{bkg}

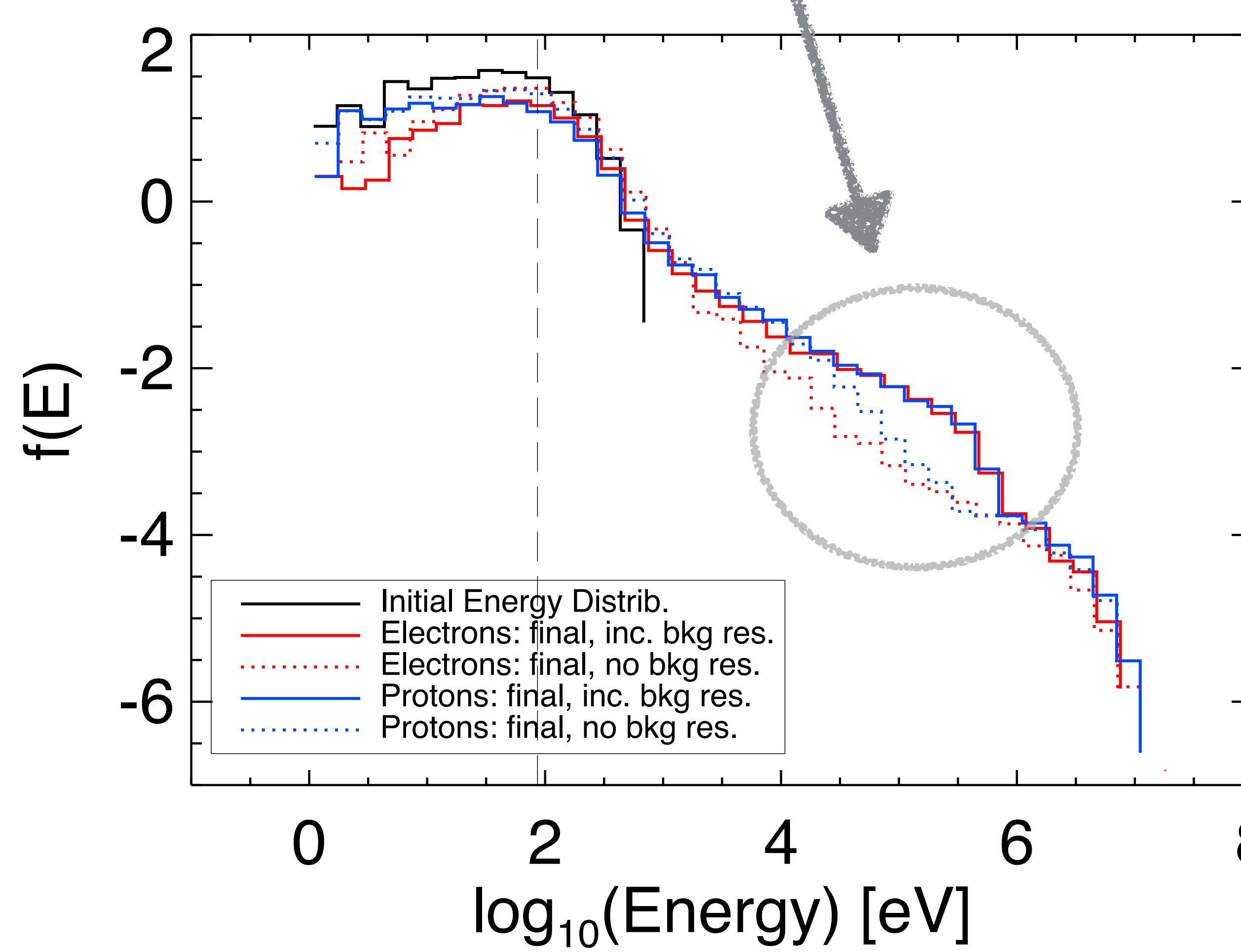

Case 1: Phase 3

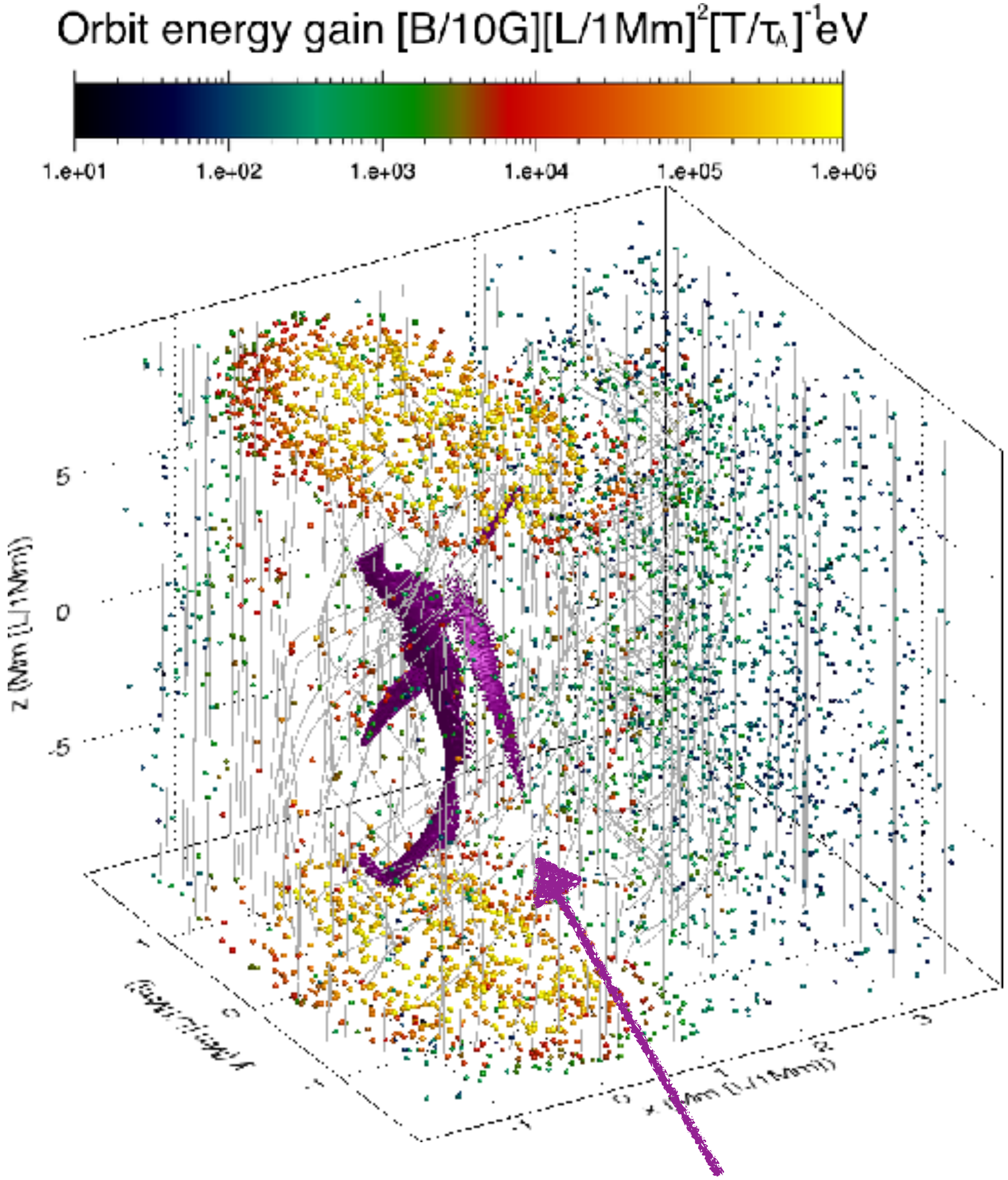

- Broader regions of accelerated orbits
- Energy dists well-matched with and without η_{bkg}:

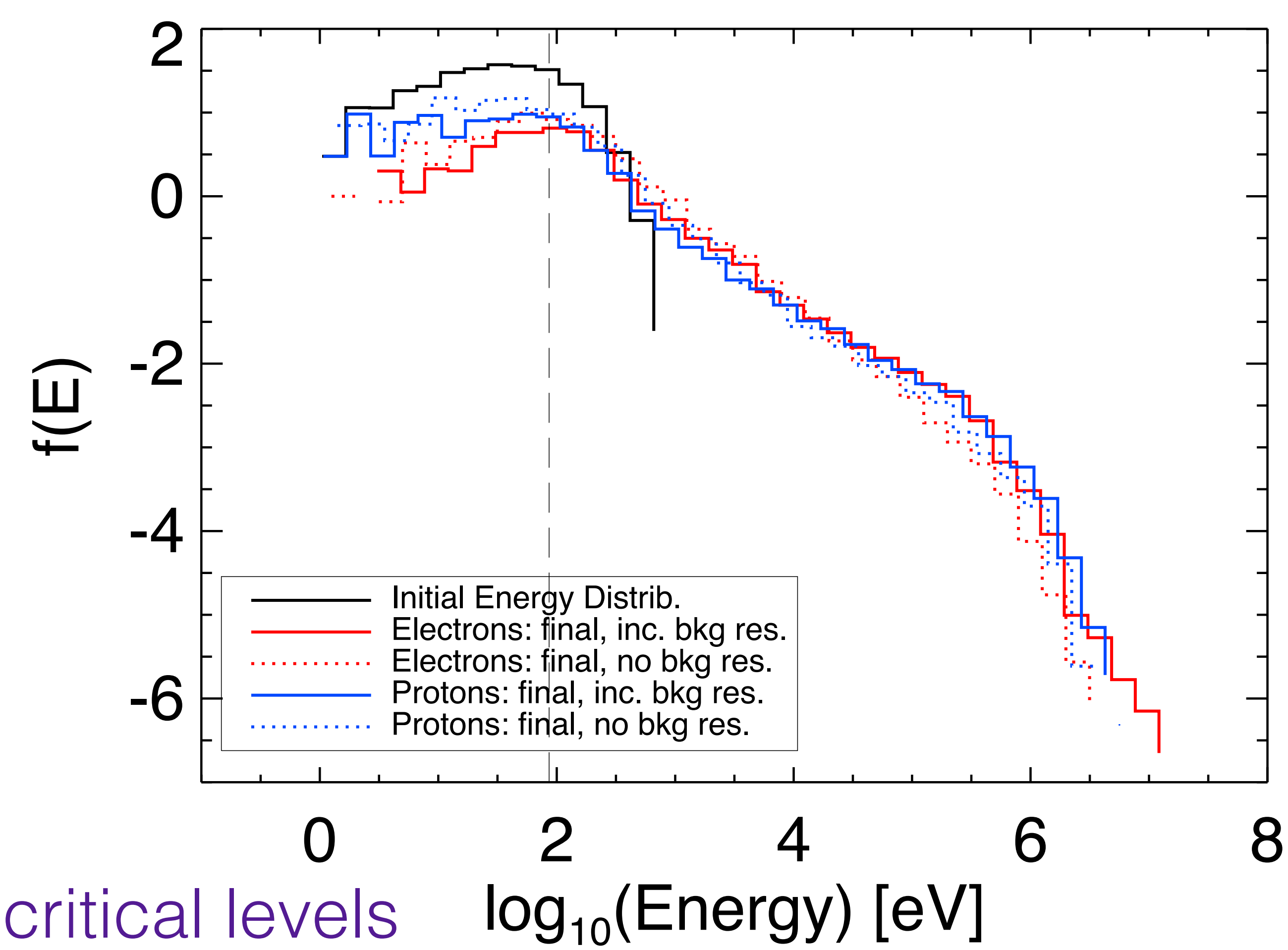

Thin current sheets rapidly dissipate to sub-critical levels

Case 2

Case 2

- How do things change when a second loop becomes destabilised?

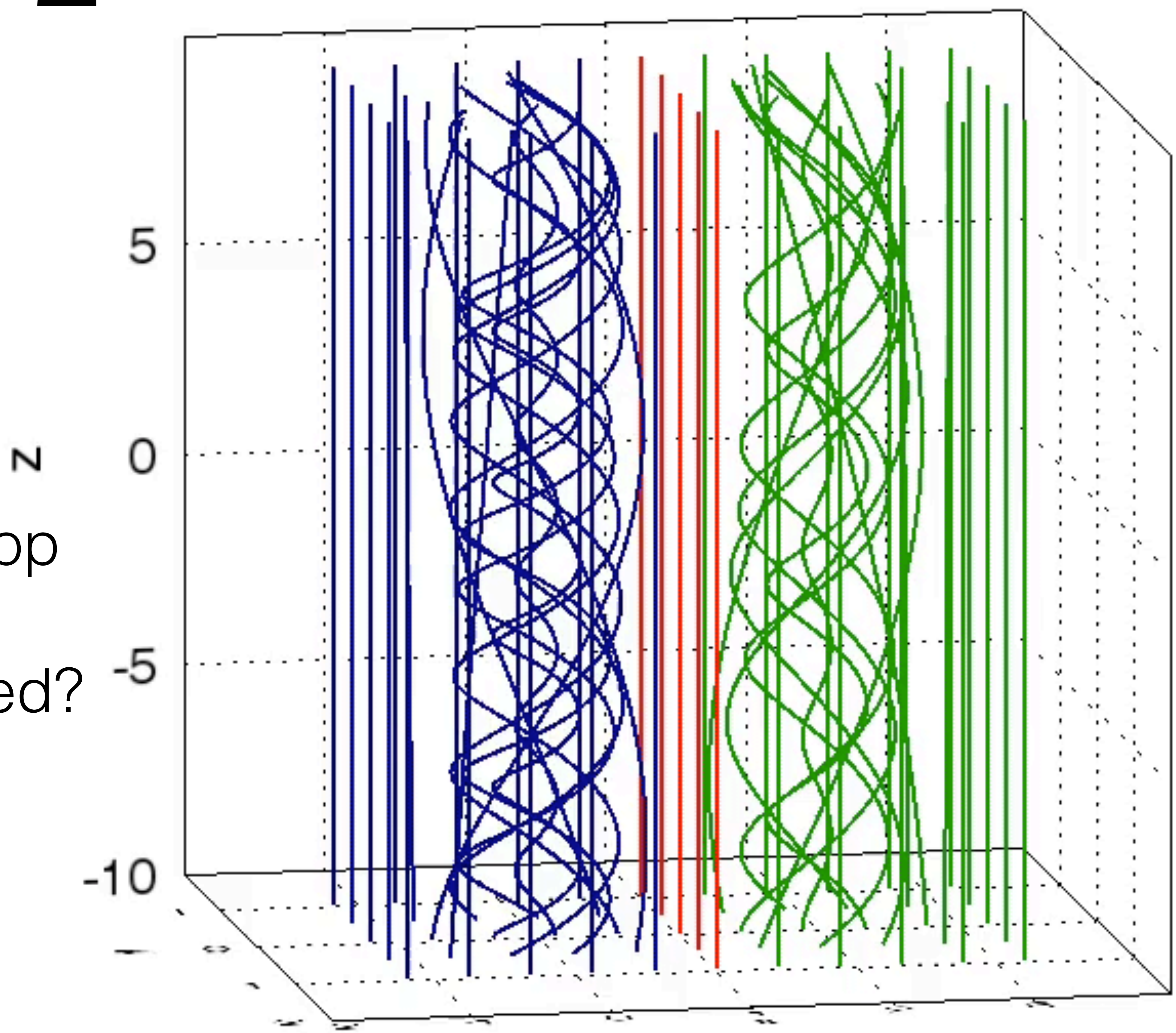

Differences between Cases

Case 1:

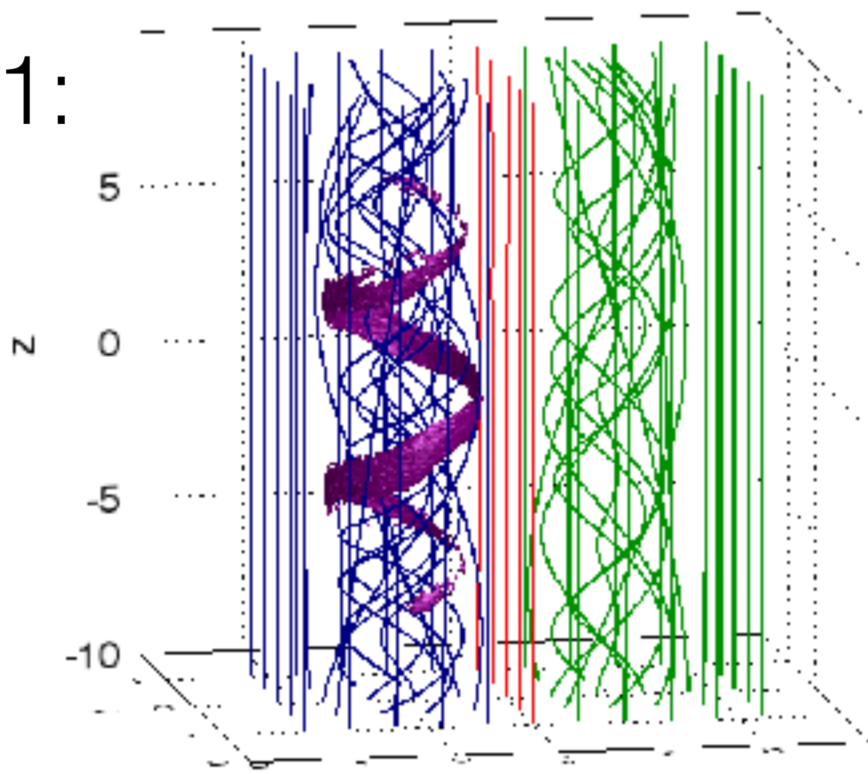

Case 2:

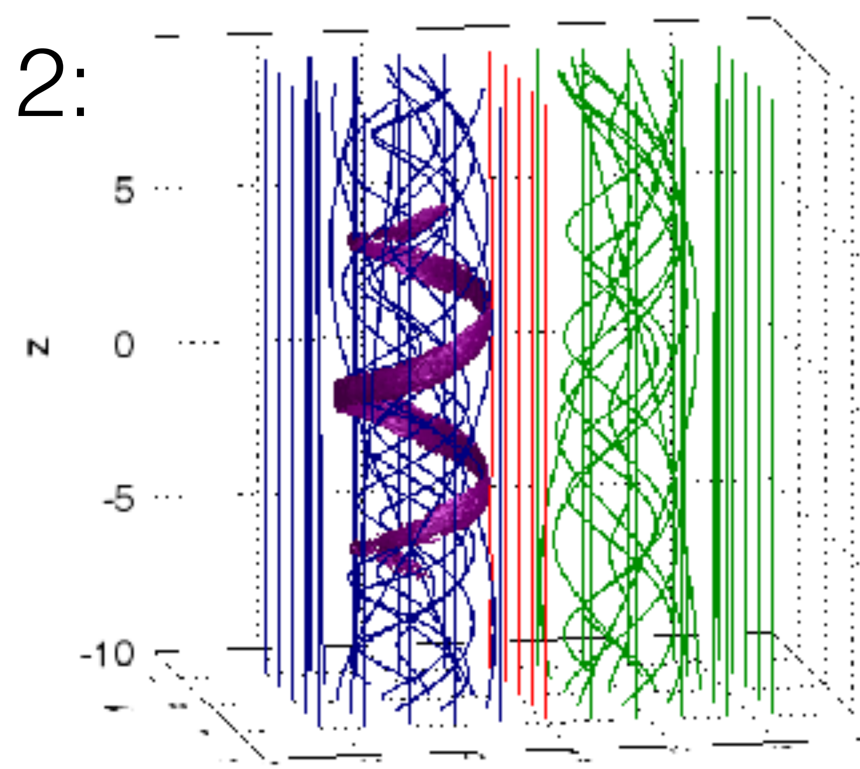

- **Secondary disruption**
- Key differences:
  - Orientation of initial helical instability
  - $\eta_{bkg}=0$
- Insert particles at multiple stages (blue arrows)

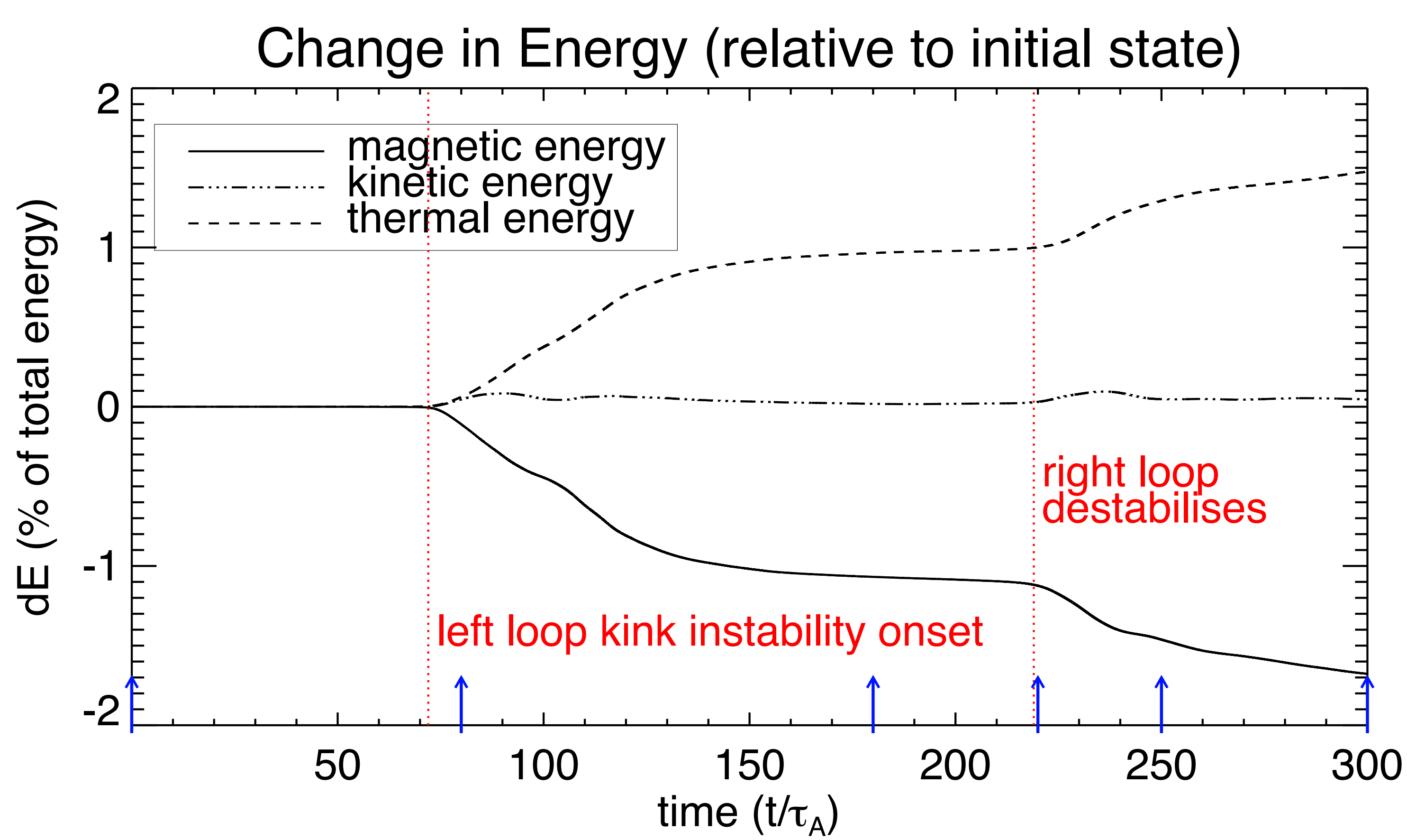

Case 2: Initial State

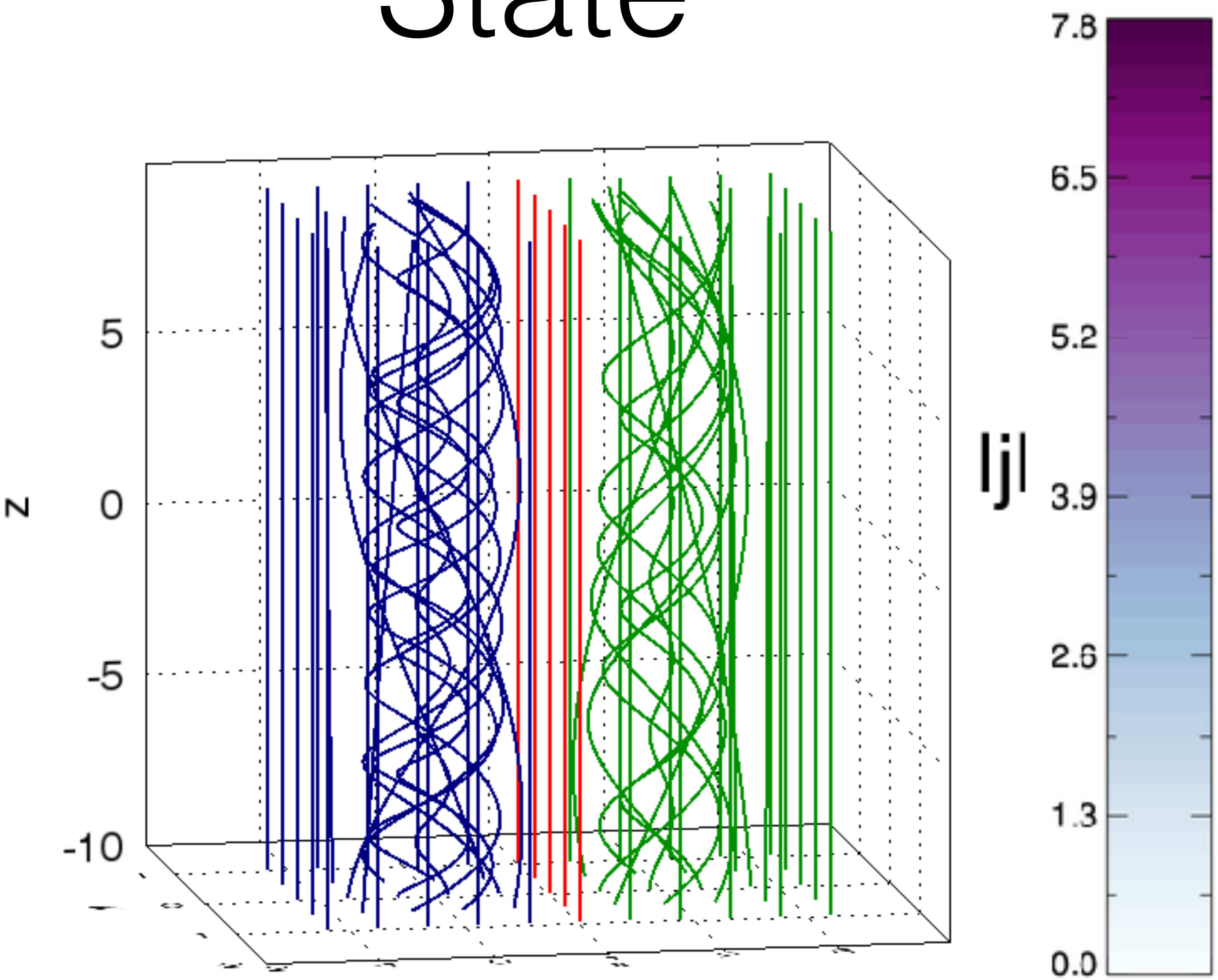

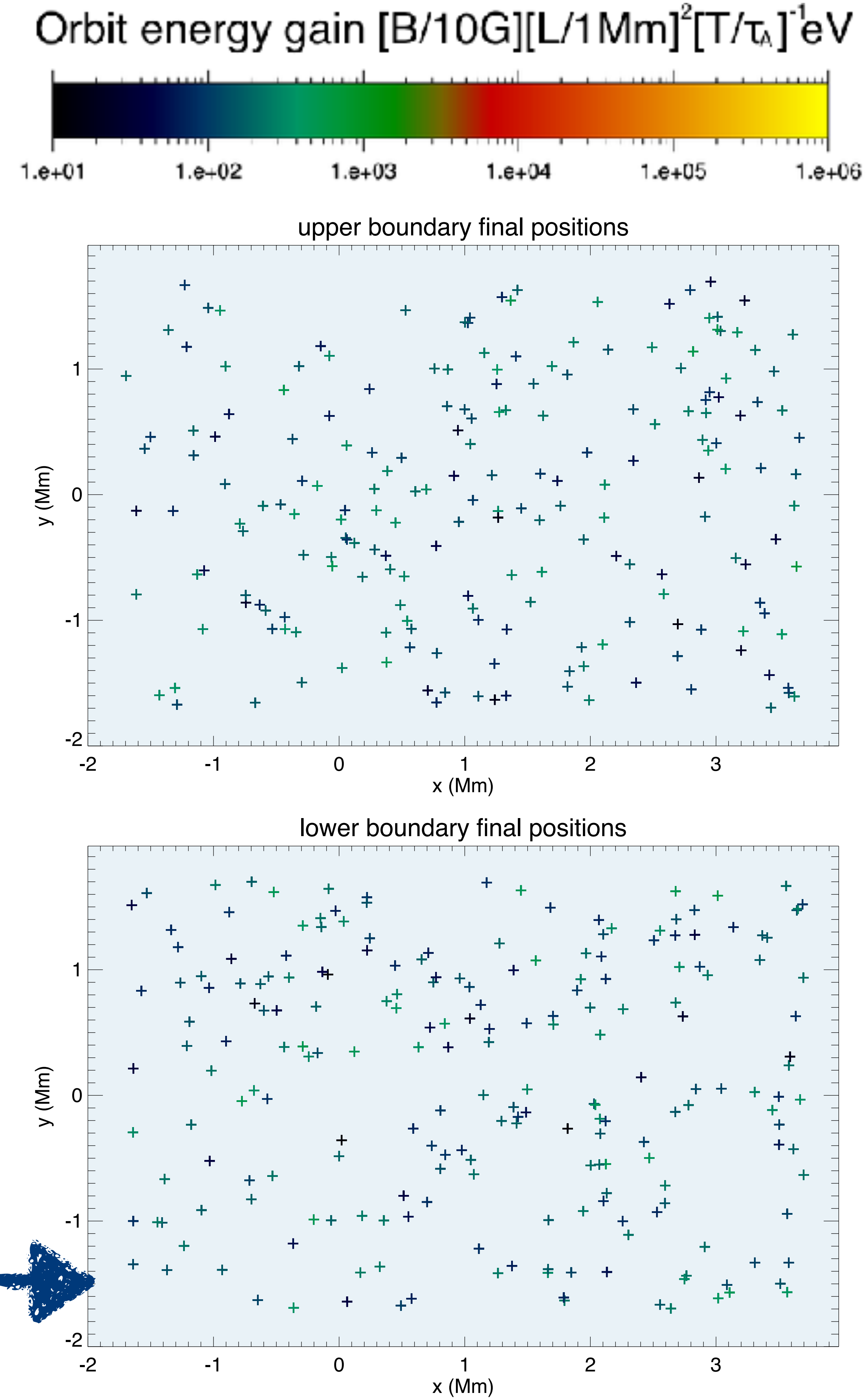

Boundary locations and midplane current |j|

Case 2: kink instability onset

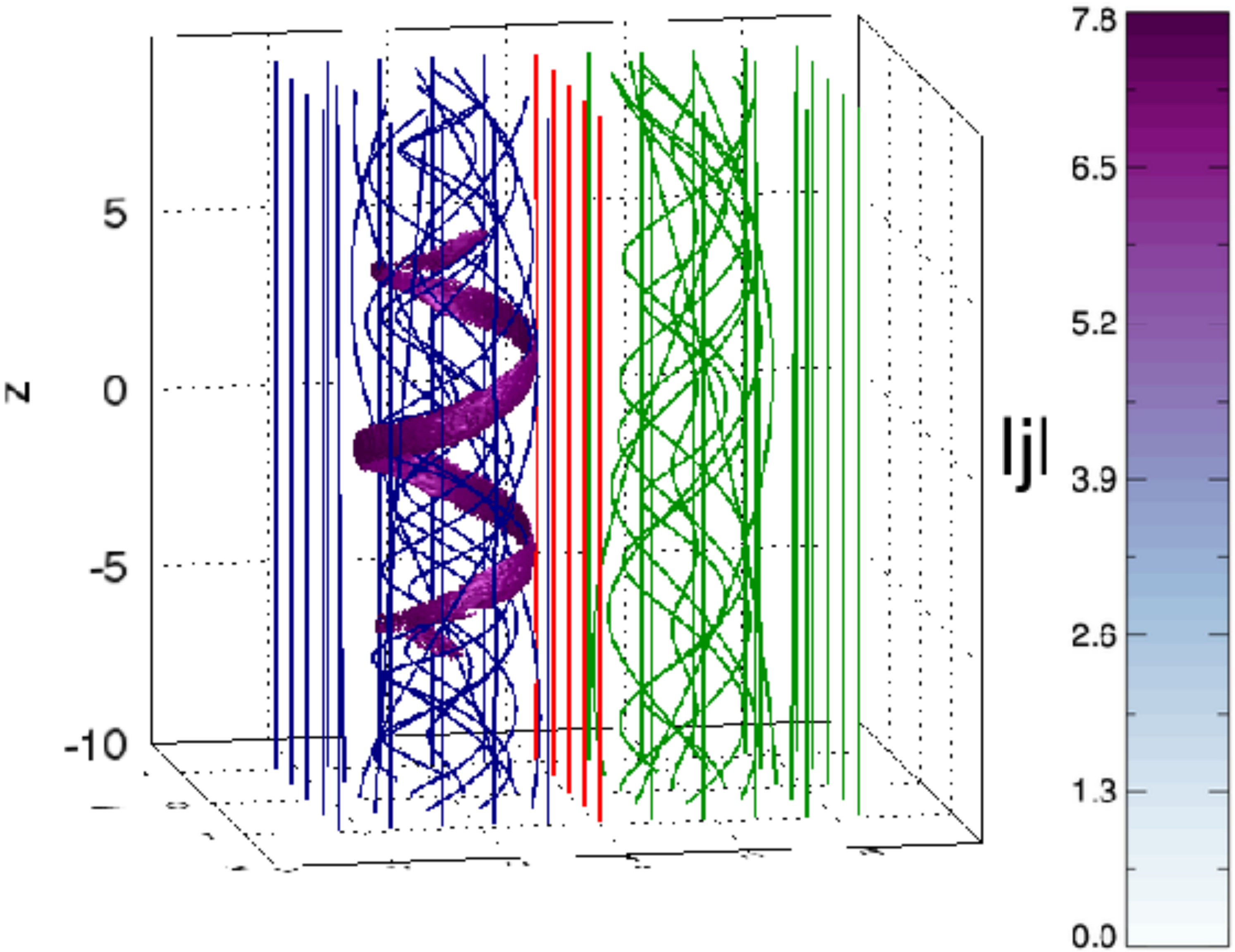

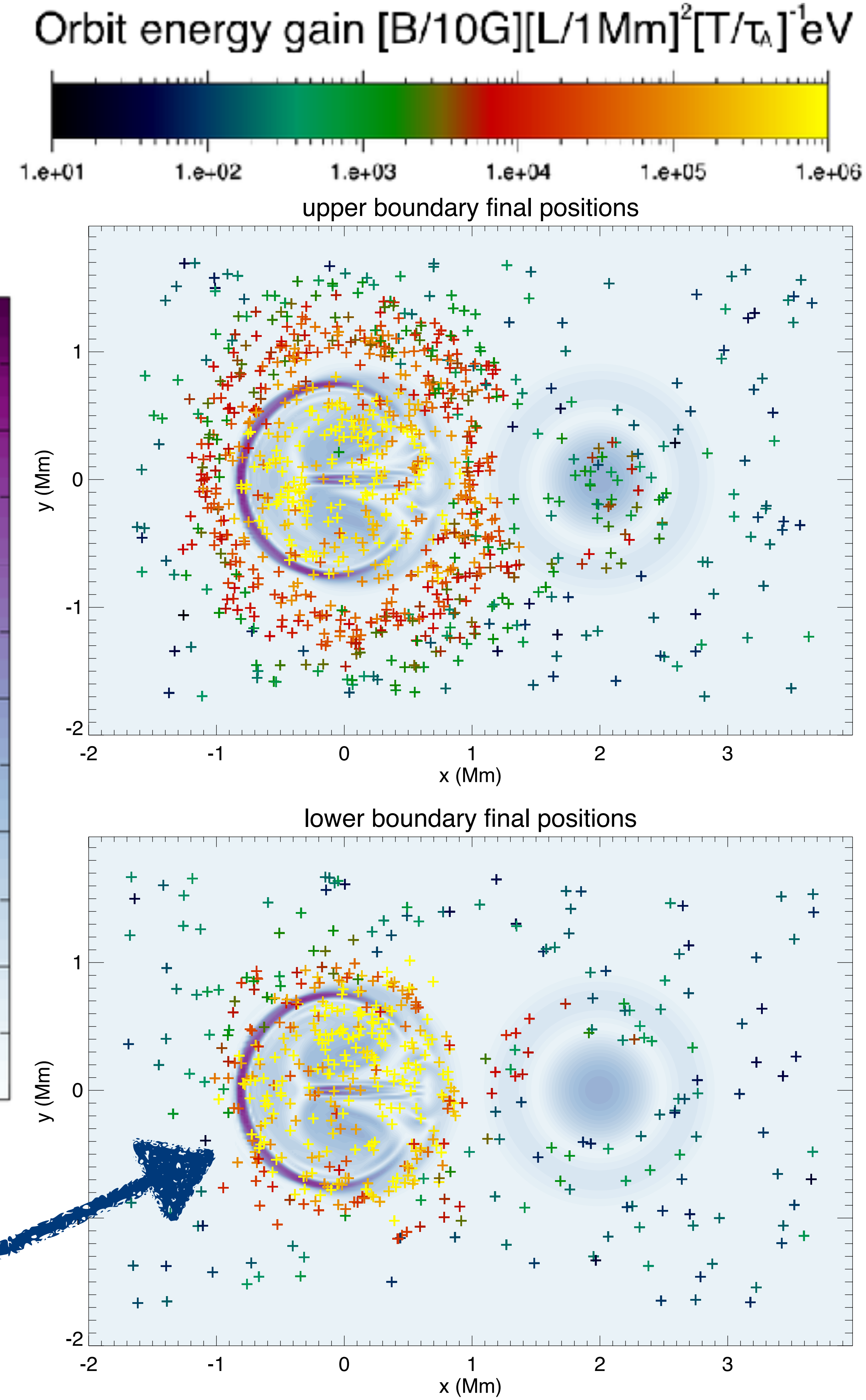

Acceleration signatures ONLY in left hand loop core

Case 2: intermediate phase

current >j_{crit} dissipates

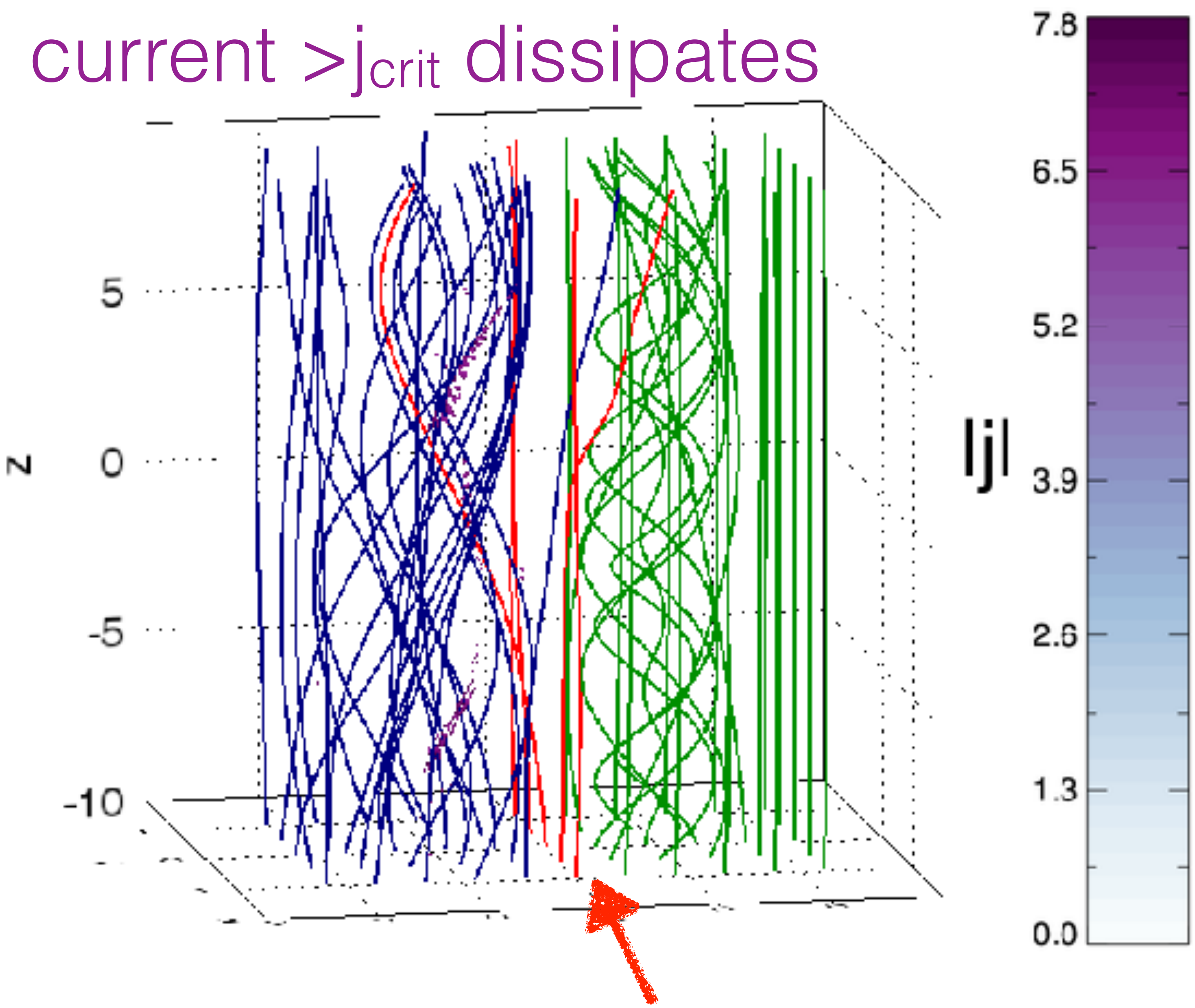

sheath field distorted

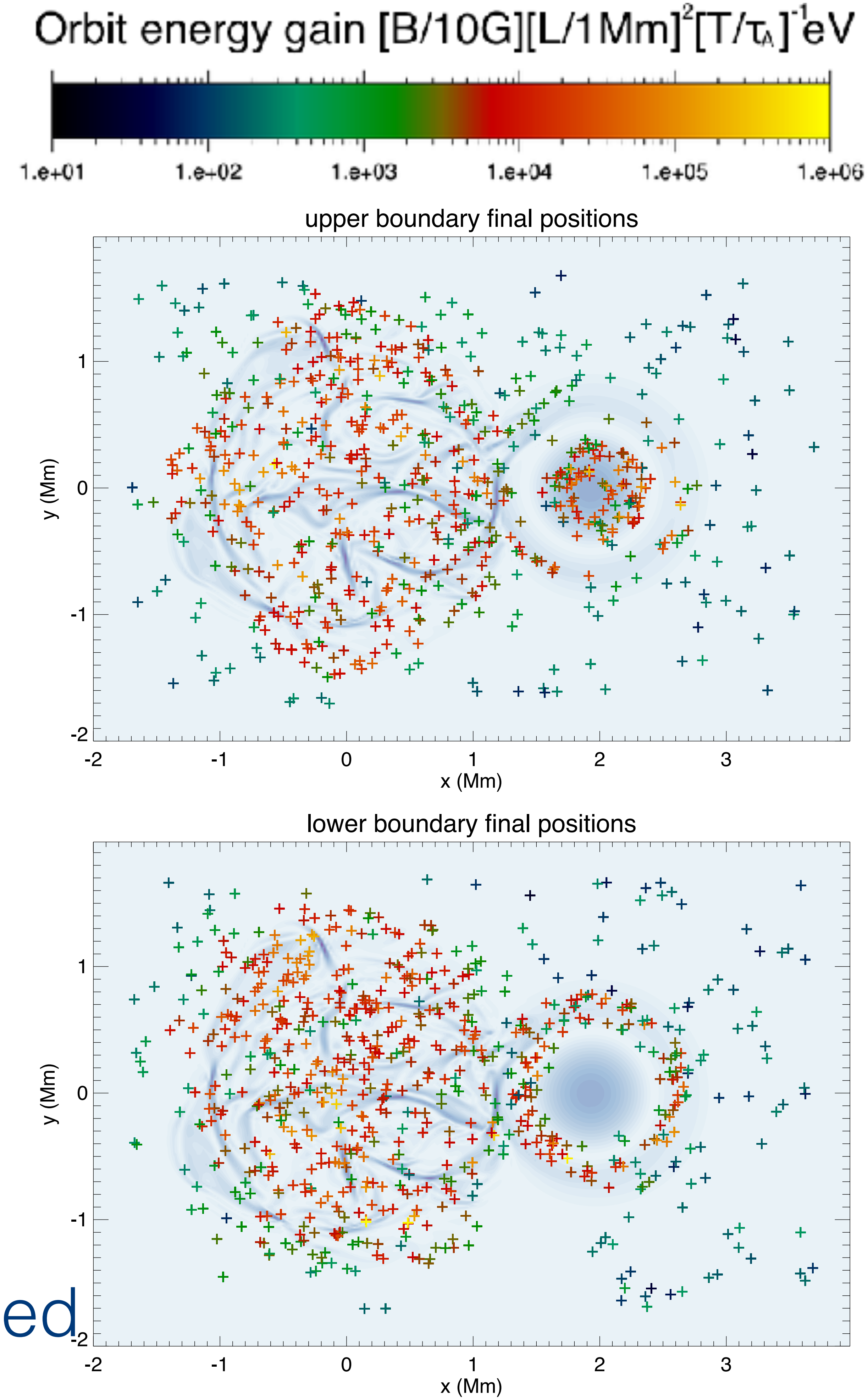

Few MeV orbits observed

Case 2: Secondary disruption

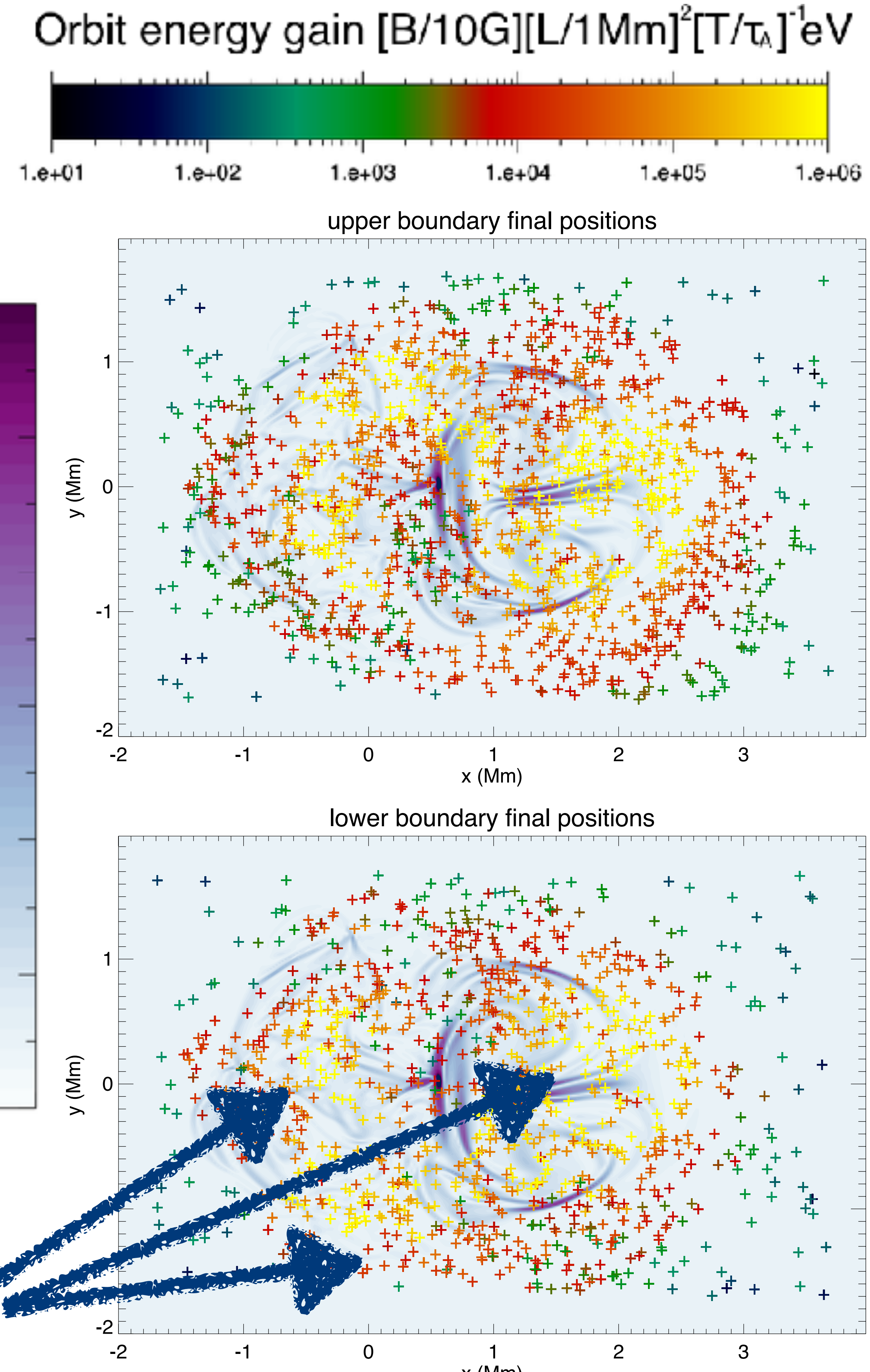

Fragmented currents >j_{crit}

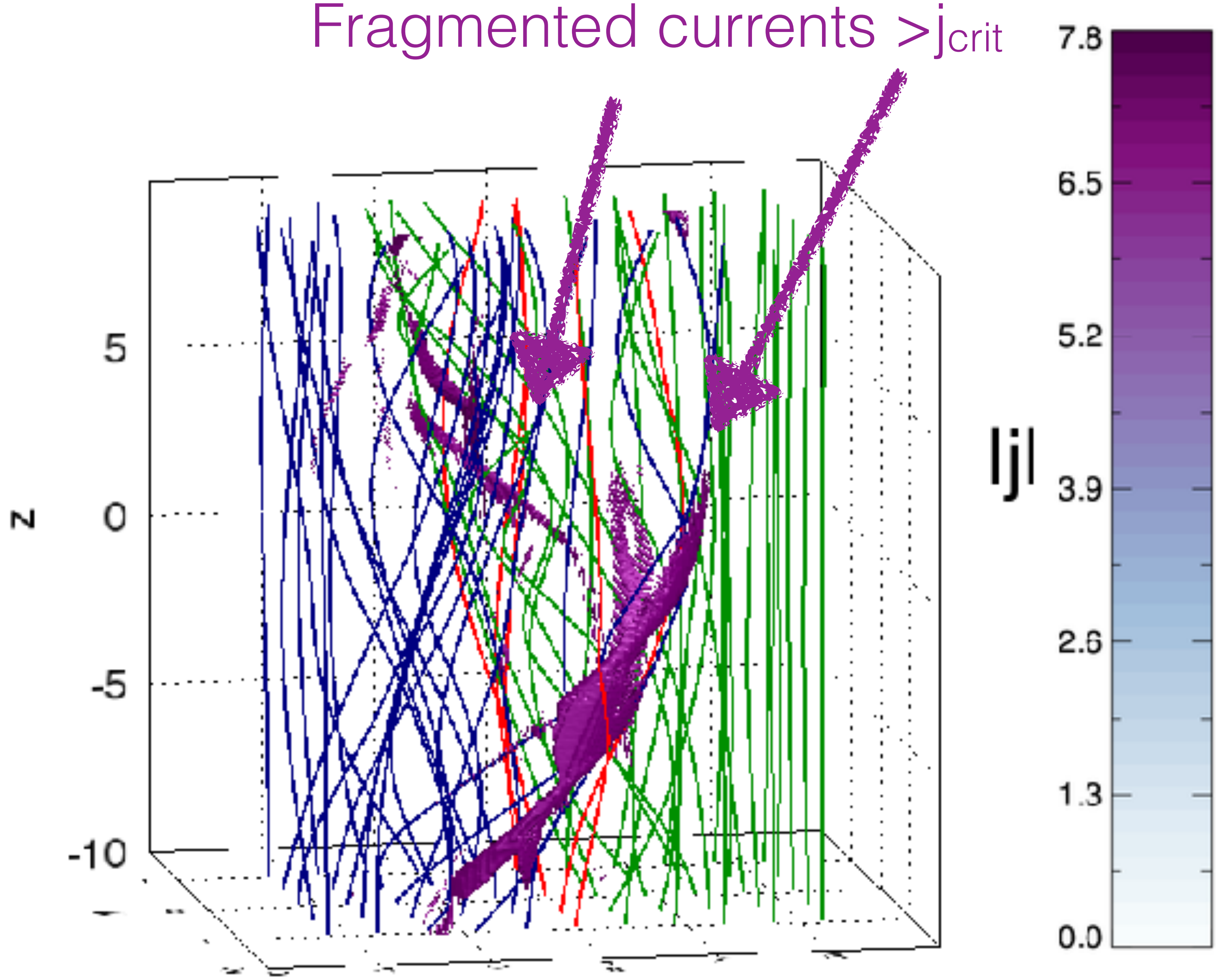

Acceleration signatures spread THROUGHOUT boundaries

Case 2: Energetics

- Proton and electron energisation nearly identical
- Energy distribs. follow reconnection rate
- Hard-soft-hard pattern for two loops
- Pattern less clear-cut if more loops included

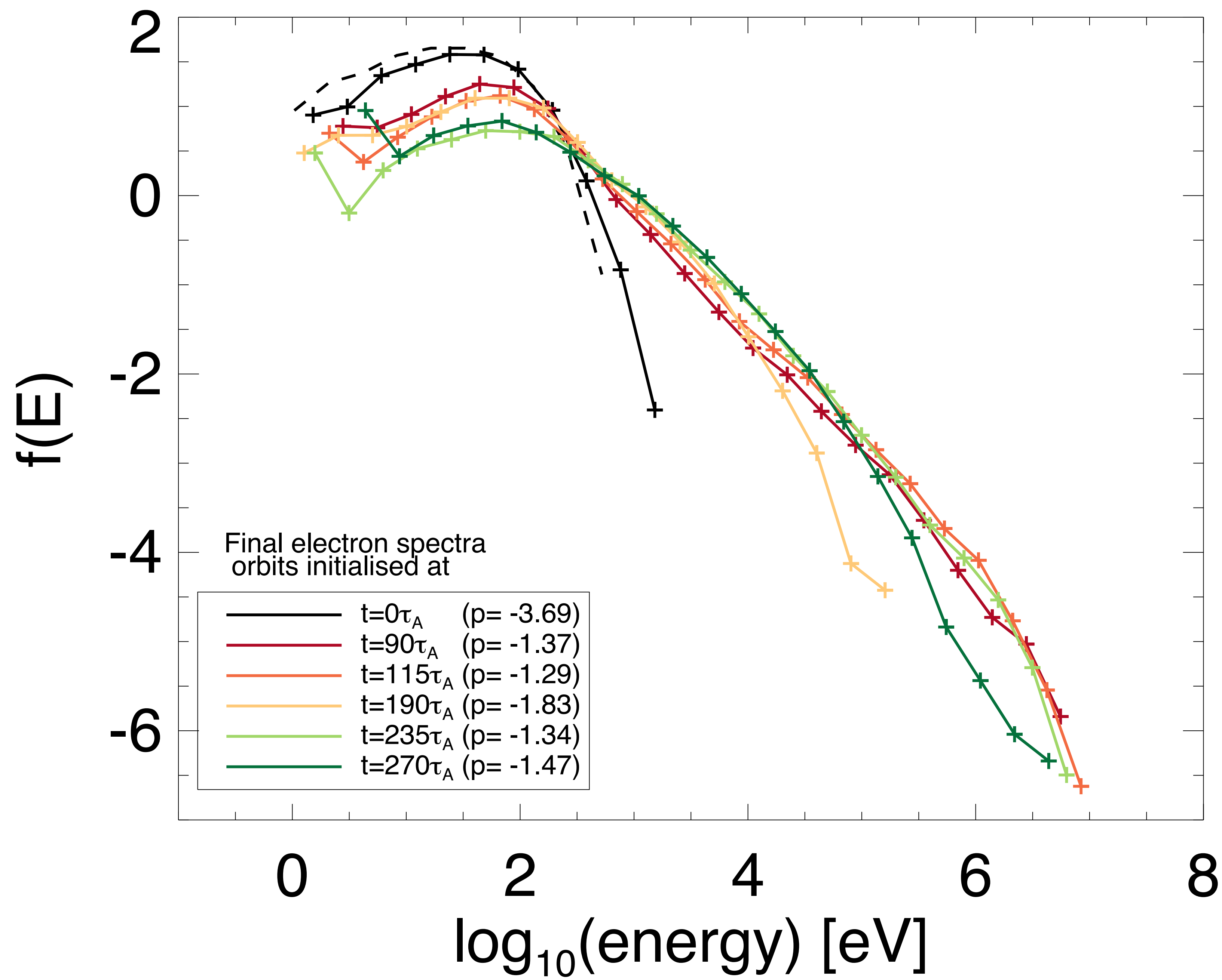

Need to improve:

- Relationship with observations (through e.g. spectra, model design, constraining coronal parameters)
- Effects of collisions and back-reaction upon global fields**

Summary

- 3D reconnection fundamentally different to 2D.
- Guiding centre theory is **not new**: careful application to 3D magnetic reconnection configurations is!
- **Parallel electric field is crucial** and sometimes overlooked!
- Multi-thread MHD loop cascade/eruption (2 loops):
  - ★ Orbit findings in single loop destabilisation align with findings of Gordovskyy et al. (2011,2012)
  - ★ Secondary loop disruption can be triggered by different orientation of helical instability.
  - ★ Energised orbit final positions fill volume of both loops during second eruption
  - ★ Spectra repeatedly harden then soften in-line with reconnection rate.

Threlfall et al., A&A, accepted (2018)
http://arxiv.org/abs/1801.02907